

RESEARCH ARTICLE

10.1002/2015MS000592

WACCM-D—Whole Atmosphere Community Climate Model with D-region ion chemistry

P. T. Verronen¹, M. E. Andersson¹, D. R. Marsh², T. Kovács³, and J. M. C. Plane³¹Earth Observation, Finnish Meteorological Institute, Helsinki, Finland, ²Atmospheric Chemistry Division, National Center for Atmospheric Research, Boulder, Colorado, USA, ³School of Chemistry, University of Leeds, Leeds, UK

Key Points:

- A selected set of D-region ion chemistry has been included in the WACCM model (WACCM-D)
- WACCM-D captures main characteristics of the lower ionosphere in various ionization conditions
- Comparison against a more extensive ion chemistry model shows agreement within tens of percent

Correspondence to:

P. T. Verronen,
pekka.verronen@fmi.fi

Citation:

Verronen, P. T., M. E. Andersson, D. R. Marsh, T. Kovács, and J. M. C. Plane (2016), WACCM-D—Whole Atmosphere Community Climate Model with D-region ion chemistry, *J. Adv. Model. Earth Syst.*, 8, 954–975, doi:10.1002/2015MS000592.

Received 23 NOV 2015

Accepted 11 MAY 2016

Accepted article online 17 MAY 2016

Published online 19 JUN 2016

Abstract Energetic particle precipitation (EPP) and ion chemistry affect the neutral composition of the polar middle atmosphere. For example, production of odd nitrogen and odd hydrogen during strong events can decrease ozone by tens of percent. However, the standard ion chemistry parameterization used in atmospheric models neglects the effects on some important species, such as nitric acid. We present WACCM-D, a variant of the Whole Atmosphere Community Climate Model, which includes a set of lower ionosphere (D-region) chemistry: 307 reactions of 20 positive ions and 21 negative ions. We consider realistic ionization scenarios and compare the WACCM-D results to those from the Sodankylä Ion and Neutral Chemistry (SIC), a state-of-the-art 1-D model of the D-region chemistry. We show that WACCM-D produces well the main characteristics of the D-region ionosphere, as well as the overall proportion of important ion groups, in agreement with SIC. Comparison of ion concentrations shows that the WACCM-D bias is typically within $\pm 10\%$ or less below 70 km. At 70–90 km, when strong altitude gradients in ionization rates and/or ion concentrations exist, the bias can be larger for some groups but is still within tens of percent. Based on the good agreement overall and the fact that part of the differences are caused by different model setups, WACCM-D provides a state-of-the-art global representation of D-region ion chemistry and is therefore expected to improve EPP modeling considerably. These improvements are demonstrated in a companion paper by Andersson et al.

1. Introduction

Recent studies of energetic particle precipitation events (EPP) have revealed significant variability in mesospheric ozone on solar cycle time scales [Andersson et al., 2014], but also the need to improve ion chemistry modeling in the D-region (i.e., altitudes < 90 km) ionosphere [Funke et al., 2011]. One of the outstanding problems, identified by the HEPPA-MMI working group (<http://heppa.iaa.es>, accessed in May, 2015), is that the observed EPP-caused changes in some important nitrogen and chlorine species cannot be represented in models. For example, HNO_3 increases measured during solar proton events (SPE) cannot be reproduced using the “standard” parameterization of HO_x ($= \text{H} + \text{OH} + \text{HO}_2$) and NO_x ($= \text{N} + \text{NO} + \text{NO}_2$) production, while models considering D-region ion chemistry in detail agree with the observations [Verronen et al., 2008, 2011]. While the HNO_3 problem can be fixed with an improved parameterization during strong precipitation events [Verronen and Lehmann, 2013], this parameterization cannot reproduce the longer-term effects of ion chemistry on reactive nitrogen partitioning, ozone, and dynamics of the middle atmosphere [Kvissel et al., 2012]. These issues have led to ion chemistry experiments in global models [Egorova et al., 2011; Krivolutsky et al., 2015], and prompted us to develop WACCM-D, a variant of the Whole Atmosphere Community Climate Model (for a description of the standard WACCM model, see Marsh et al. [2013] and references therein), which incorporates a set of D-region ion chemistry with the aim to produce the observed EPP effects in the mesosphere and upper stratosphere.

A concern with including the D-region chemistry in 3-D atmospheric models has been the large number of ionic species and their reactions that exist in the lower ionosphere. For example, in an extensive model such as the Sodankylä Ion and Neutral Chemistry (SIC) model [Verronen et al., 2005], there are over 70 ions and 400 ion-neutral reactions, and over 2000 ion-ion recombination reactions. Such an increase in species and reactions might require too much computing resources and make simulations too slow and thus impractical. Another issue has been the very short chemical lifetime of ions which makes chemical reaction

© 2016. The Authors.

This is an open access article under the terms of the Creative Commons Attribution-NonCommercial-NoDerivs License, which permits use and distribution in any medium, provided the original work is properly cited, the use is non-commercial and no modifications or adaptations are made.

systems stiffer and thus slower to simulate because shorter time steps are required. These issues, in general, remain today. However, as we will show in the following, current computing resources and chemistry solvers are such that neither issue is critical for detailed (i.e., not complete but adequate for EPP) and global ion chemistry modeling.

In this paper, we present WACCM-D, compare its ionospheric results to those from the SIC model, and discuss the differences. We consider selected ionization scenarios from midlatitudes to the polar regions, including the extreme case of the January 2005 solar proton event (SPE) [e.g., *Verronen et al.*, 2006a; *Jackman et al.*, 2011]. In a companion paper (M. E. Andersson et al., WACCM-D—Improved modeling of nitric acid and active chlorine during energetic particle precipitation, submitted to *Journal of Geophysical Research*, 2016), the WACCM-D SPE effects on neutral species, such as ozone and nitric acid, are compared to satellite observations.

2. Sodankylä Ion and Neutral Chemistry Model

The SIC model is a 1-D model designed for ionosphere-neutral atmosphere interaction studies. The latest chemical scheme includes 70 ions, of which 41 are positive and 29 negative. Of the 34 neutral species included, 16 belonging to the oxygen (O , $O(^1D)$, $O(^1\Delta_g)$, O_3), hydrogen (H , OH , HO_2 , H_2O_2), and nitrogen ($N(^4S)$, $N(^2D)$, NO , NO_2 , NO_3 , N_2O_5 , HNO_2 , HNO_3) families are solved in the model while the rest are taken as background. The altitude range of SIC is from 20 to 150 km, and the chemical time step is 15 min. The model takes into account external forcing due to solar UV and soft X-ray radiation, electron and proton precipitation, and galactic cosmic rays. A detailed description of SIC is given, e.g., by *Verronen et al.* [2005] and *Turunen et al.* [2009]. Note that SIC has been shown to produce well both ionospheric and neutral atmospheric changes observed during EPP events [*Verronen et al.*, 2005, 2006a, 2006b, 2008, 2011, 2015].

In the WACCM-D development, SIC has been used as an ion chemistry guide on which the selected set of WACCM-D ion chemistry is based. On the other hand, in this paper, SIC is also used as a reference to assess the quality of the WACCM-D results produced with the reduced ion chemistry. Because the models are very different (a 1-D chemistry model, and a 3-D chemistry-climate model), we restrict ourselves to comparing only the electron and ion concentrations between the models. The comparison to SIC gives very useful information about the quality of the WACCM-D lower ionosphere. However, the model-to-model comparison of detailed ion composition (e.g., concentrations of individual ions) is perhaps not a direct measure of WACCM-D quality, considering that relatively little detailed information is available from observations (to validate SIC). A more significant test of WACCM-D ion chemistry is to compare the modeled, EPP-caused changes in neutral species against satellite observations. This comparison is done in a companion paper (Andersson et al., submitted manuscript, 2016).

3. WACCM

The Whole Atmosphere Community Climate Model (WACCM) is a global, 3-D climate model developed by the National Center for Atmospheric Research (NCAR) that spans the range of altitude from Earth's surface to the thermosphere (up to $\approx 6 \times 10^{-6}$ hPa, ≈ 140 km) [*Marsh et al.*, 2013, and references therein]. WACCM is an extension of the Community Atmosphere Model that includes fully interactive chemistry, radiation, and dynamics [*Neale et al.*, 2012]. Version 4 with preconfigured specific dynamics scenario (SD-WACCM) has 88 vertical levels and is forced with GEOS5.1 reanalysis data [*Reinecker et al.*, 2008] below 50 km (fully interactive above). Horizontal resolution is 1.9° latitude by 2.5° longitude. The vertical resolution varies from 1.1 km in the troposphere, 1.1–2 km in the stratosphere to ≈ 3.5 km in the mesosphere and lower thermosphere. WACCM includes a detailed neutral chemistry model for the atmosphere based on the Model for Ozone and Related Chemical Tracers (MOZART) that represents chemical and physical processes in the troposphere through the lower thermosphere [*Kinnison et al.*, 2007]. WACCM contains an ion chemistry model which represents the ionospheric E-region and consists of six constituents (O^+ , O_2^+ , N^+ , N_2^+ , NO^+ , and electrons). A description of the included ion-neutral and recombination reactions can be found in *Neale et al.* [2012, section 5.6.7]. The system of time-dependent Ordinary Differential Equations (ODE) is solved for chemically long-lived and short-lived species using the Explicit Forward Euler method and the Implicit Backward Euler method, respectively [*Sandu et al.*, 1996]. The chemical time step is 30 min. Ionization sources include absorption of extreme ultraviolet and soft X-ray photons, photoelectron impact, and parameterization of energetic particles precipitation in

Table 1. WACCM-D: Initial Production Rates of Ions and Neutral Species Due to SPE

Product	Rate	Reference
$P(N_2^+)$	$0.585 \times Q^a$	Rusch et al. [1981]
$P(N^+)$	$0.185 \times Q$	Rusch et al. [1981]
$P(N(^4S))$	$0.502 \times Q$	Total $P(N, N^+)$ [Porter et al., 1976] - $P(N^+)$ [Rusch et al., 1981], $N(^4S)/N(^2D)$ branching from Zipf et al. [1980] (scaled)
$P(N(^2D))$	$0.583 \times Q$	As $P(N(^4S))$
$P(O_2^+)$	$0.154 \times Q$	Rusch et al. [1981]
$P(O^+)$	$0.076 \times Q$	Rusch et al. [1981]
$P(O)$	$1.074 \times Q$	Total $P(O, O^+)$ [Porter et al., 1976] - $P(O^+)$ [Rusch et al., 1981]

^a Q = total SPE ionization rate ($cm^{-3} s^{-1}$).

the auroral regions based on the Thermosphere-Ionosphere-Mesosphere-Electrodynamics General Circulation Model (TIME-GCM) [Roble and Ridley, 1987]. The atmospheric ionization rates due to solar protons are calculated and applied at altitudes below ≈ 108 km based on GOES data available from the National Oceanic and Atmospheric Administration (NOAA) Space Environment Center (<http://sec.noaa.gov/Data/goes.html>) and the methodology discussed in Jackman et al. [2009]. The HO_x production due to SPEs uses a lookup table from Jackman et al. [2005], which is based on the work of Solomon et al. [1981]. For NO_x , it is assumed that 1.25 N atoms are produced per ion pair with branching ratios of 0.55/0.70 for $N(^4S)/N(^2D)$, respectively [Jackman et al., 2005; Porter et al., 1976]. Galactic cosmic ray ionization is not currently included in WACCM.

4. WACCM-D

WACCM-D is a variant of the Whole Atmosphere Community Climate Model, which incorporates a set of D-region ion chemistry with the aim to produce the observed effects of EPP in the mesosphere and stratosphere. In the following, we describe the new features of WACCM-D. The original WACCM 5-ion chemistry, including the photoionization and auroral ionization processes, are unchanged, included in WACCM-D, and described in detail in Marsh et al. [2007].

4.1. Initial Production of Ions and Neutrals

For the SPE modeling, the WACCM method of parameterized HO_x and NO_x production was replaced by initial production rates of ions and neutrals due to particle impact ionization, dissociative ionization, and secondary electron dissociation. These are calculated from the total ion pair production rate as shown in Table 1, based on the work of Porter et al. [1976], Zipf et al. [1980], and Rusch et al. [1981]. It should be noted that the initial production rates given in Table 1 were calculated for the homosphere, i.e., assuming a fixed N_2/O_2 ratio and neglecting direct ionization of atomic oxygen [Sinnhuber et al., 2012, section 2.2.1]. However, the bulk of SPE ionization is at altitudes below 90 km where they are valid.

4.2. Ions and Ionic Reactions

We emphasize that the D-region ion chemistry is not included in WACCM-D as a separate module, but the new ions and reactions are simply added to the standard WACCM chemistry scheme. This approach is straightforward and benefits from the optimized, validated ODE chemistry solver of WACCM [Sandu et al., 1996]. The solver is able to handle the ions as “normal” species without numerical problems, despite some ions having very short lifetimes and making the chemical system stiffer.

Table 2. The Number of Ionic Reactions in WACCM-D and the Reduction, in Percent, Compared to the Full Scheme of SIC

Reaction Group	WACCM-D	Reduction
Positive ion reactions	46	60%
Recombination of positive ions with electrons	16	45%
Photodetachment of positive ions	1	0%
Electron attachment on neutrals	3	0%
Negative ion reactions	90	27%
Electron detachment from negative ions	14	0%
Photodetachment of electrons from negative ions	6	14%
Photodissociation of negative ions	5	0%
Positive ion-negative ion recombination	129	94%

The WACCM-D ion reaction schemes are based on those from the SIC model, although a considerable number of ions and reactions have been excluded (see Table 2 for detailed numbers). Included are the ions and reaction paths that are essential to represent the effects on the HO_x and NO_y neutral species during EPP forcing, the selection is based on the detailed analysis by Verronen and Lehmann [2013]. For example, the reaction paths leading to $H^+(H_2O)_n$ and $NO_3^-(HNO_3)_n$ type ions (here n is the

production due to SPEs uses a lookup

table from Jackman et al. [2005], which is based on the work of Solomon et al. [1981]. For NO_x , it is assumed that 1.25 N atoms are produced per ion pair with branching ratios of 0.55/0.70 for $N(^4S)/N(^2D)$, respectively [Jackman et al., 2005; Porter et al., 1976]. Galactic cosmic ray ionization is not currently included in WACCM.

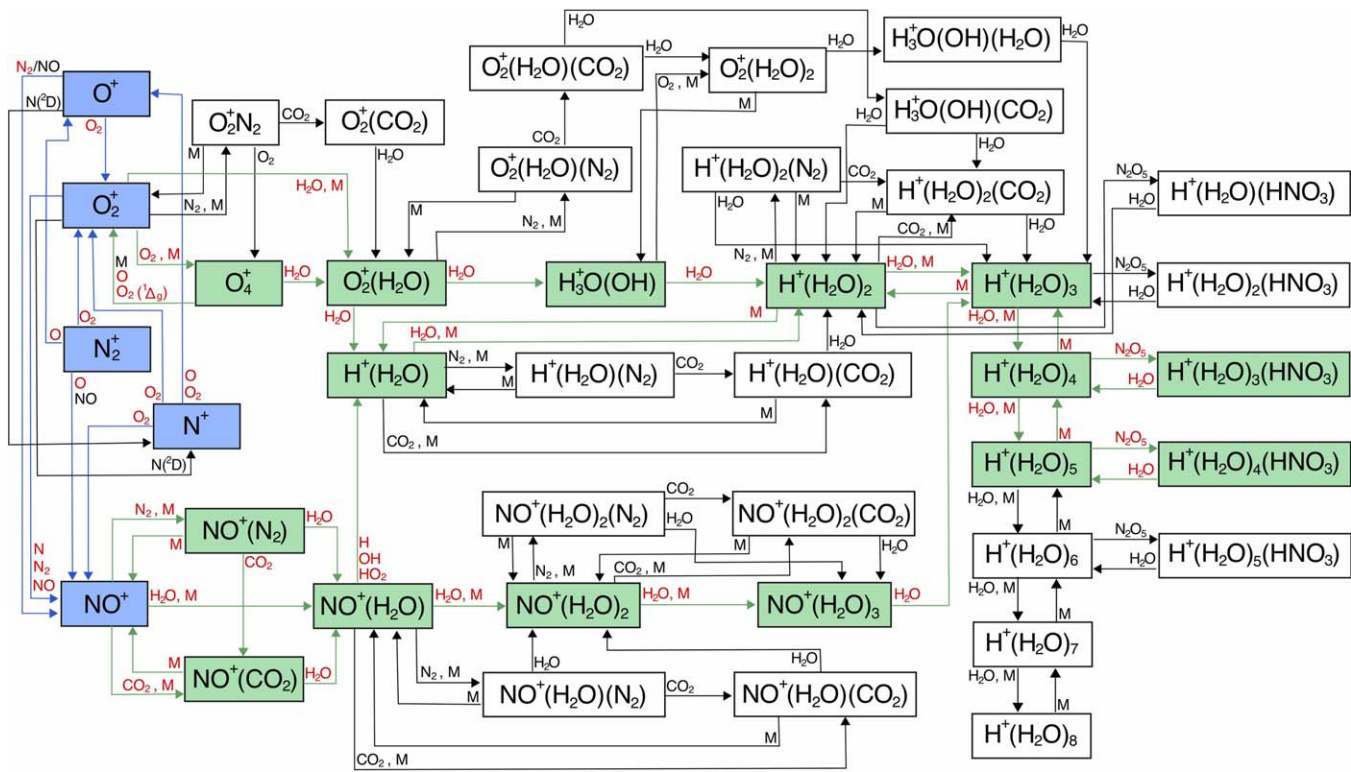
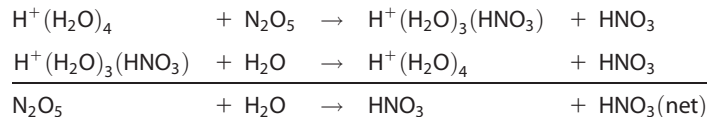


Figure 1. Positive ion reaction scheme of the SIC model. The colors indicate the subsets included in WACCM (blue) and WACCM-D (blue and green).

order of clustering, i.e., 0, 1, 2, etc.) are included so that HNO₃ can be produced from NO_x. Also, two reaction sequences such as



have been included so that the ionic N₂O₅-to-HNO₃ conversion in the winter polar region can be modeled [e.g., Kvissel et al., 2012, and references therein]. A comparison between the ion chemistry schemes in WACCM-D and SIC is shown in Figures 1 and 2. The total number of positive ions, negative ions, and ion reactions incorporated to WACCM-D are 20, 21, and 307, respectively. The full lists of ions, ionic reactions, and reaction rate coefficients included in WACCM-D are given in the Appendix A.

The ion-electron and ion-ion recombination (IIR) reactions are not shown in Figures 1 and 2, although they are included in the total of 307 WACCM-D ionic reactions. The complete number of IIR reactions for the SIC ion set would have been 2254 (there is both a two-body and a three-body reaction for each positive-negative ion pair). To reduce this number, IIR was included only for the most abundant terminal ions (7 positive, 16 negative for the two-body recombination, 2 positive and 7 negative for three-body recombination), as listed in the Appendix A, and not considered for the other ions. Note that the neutral products of some of the IIR reactions are not known from the scientific literature [Verronen and Lehmann, 2013]. In those cases, an educated guess is used to complete the reactions. However, the products of the most important IIR reactions are known. Also, the uncertainty about those of the other IIR reactions should have no significant direct effects on ion composition because neutral species are produced. In principle, neglecting IIR loss for some ions in WACCM-D could lead to problems such as accumulation of charge. However, these ions do not live forever in the model, they are simply converted to the terminal ions that are then lost through IIR. Finally, any inaccuracy caused by this approach will be included in the total differences between WACCM-D and SIC (the differences are presented in section 6).

The D-region ion chemistry is included in WACCM-D over its whole altitude range, technically in the same way as all other chemistry. However, as will be shown in the following sections, positive cluster ions and

Table 3. The Ionization Scenarios^a

Scenario	Latitude	Solar Radiation	GCR/SPE
SC1	40°N	As in WACCM	GCR (fixed)
SC2	70°N	As in WACCM	GCR (fixed) + SPE (Jackman)

^aGCR (fixed altitude profile, no change with time) was applied at all latitudes, SPE at geomagnetic latitudes larger than 60°E

polar regions in mid-January, and the related ionization rates exceeded $10^3 \text{ cm}^{-3} \text{ s}^{-1}$ above 50 km during peak forcing. Considering an SPE case allows us to investigate the model behavior when extreme ionization covers most of the middle atmosphere. The ionization rates for the SPE event are the daily data provided by C. H.

Jackman and used in WACCM by default (available at <http://solarisheppa.geomar.de/solarprotonfluxes>, accessed in May, 2015). Other ionization sources included are solar EUV radiation and galactic cosmic radiation (GCR). EUV ionization (shown from 40°N) exceeds $10^{-2} \text{ cm}^{-3} \text{ s}^{-1}$ only during the daytime hours at altitudes above 65 km, reaching to $\approx 100 \text{ cm}^{-3} \text{ s}^{-1}$ at 90 km, while the ionization rate due to GCR at 20 km is about $25 \text{ cm}^{-3} \text{ s}^{-1}$ and decreases with altitude to values less than $10^{-2} \text{ cm}^{-3} \text{ s}^{-1}$ above 55 km.

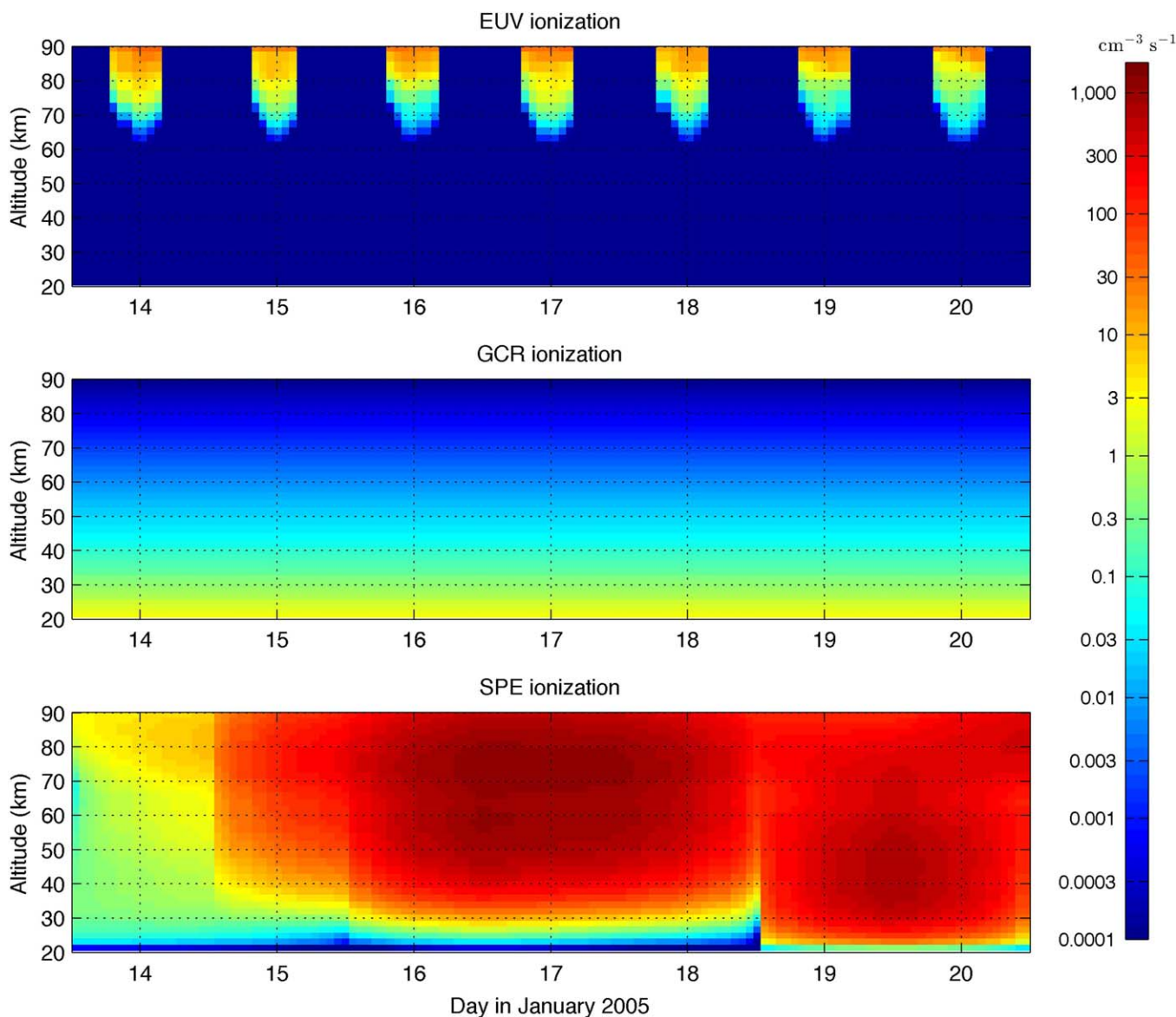


Figure 3. Ionization rates due to (top) solar EUV and Lyman- α radiation at 40N, (middle) GCR as applied at all latitudes, and (bottom) SPE applied at geomagnetic latitudes $\geq 60^\circ$. x axis tick marks are at noon each day.

Our version of WACCM-D (or WACCM) does not include ionization by GCR, the sole constant source of ionization at altitudes below about 65 km at low and middle latitudes. Thus, except for the SPE-affected polar regions, the results from WACCM-D in the lower middle atmosphere would not be realistic. Although comparison with SIC (after switching off GCR) would in principle be possible, we found that the models cannot handle unrealistic conditions of zero ionization (not shown). For this reason, GCR is included as a fixed altitude profile (i.e., the ionization rate varies with altitude but not in time), as shown in Figure 3 (middle). The same altitude profile was used in both SIC and WACCM-D, by adding the GCR ionization rates to those of the SPE. This is a reasonable approach which helps us to avoid problems caused by zero ionization outside polar latitudes.

Note that we include GCR in this simplified manner for purposes of our model-model comparison only. Notably, our GCR input includes no latitudinal dependence. However, for the purpose of our paper, it is more important to force WACCM-D and SIC with the same GCR than to describe the relatively small latitudinal variability correctly. Very recently, a proper GCR scheme has become available for WACCM [Jackman *et al.*, 2015], and it will be implemented in WACCM-D in the near future.

5.2. Simulations

WACCM-D, driven by GEOS5.1 meteorology, was run for the time period 1–31 January 2005. SPE and GCR ionization rates were applied at geomagnetic latitudes $>60^\circ$ and globally, respectively. Output was written every hour, instantaneously. Note that the addition of 292 D-region ion reactions (to the original WACCM 5-ion scheme of 15 reactions, making a total of 307 reactions) resulted in about 100% increase in computing time (WACCM-D compared to WACCM).

As an example of WACCM-D output, Figure 4 shows the global electron concentration on 17 January (midnight UT) at 69 and 87 km altitude. Due to strong SPE ionization, the polar latitudes above 60° (geomagnetic) show largest amounts of electrons. At lower latitudes, a clear diurnal variability is seen due to solar EUV radiation which increases the electron concentration during daytime, while at night, GCR is the dominant ionization source. In the Northern Hemisphere at 69 km, the sunlit region influenced by SPE (at 120° – 270° longitude, 50°N – 75°N latitude) has a larger electron concentration compared to nighttime SPE regions due to solar radiation affecting the balance between electrons and negative ions at altitudes below about 80 km [e.g., Verronen *et al.*, 2006b]. At 87 km, an interesting feature in the mid and low latitudes is the decrease around sunset which does not fully reflect the fast decrease in EUV ionization (like sunrise does) but shows a more gradual change which seems to be influenced by atmospheric dynamics.

The SIC simulations were done for the time period of 14–20 January 2005, at two geographical latitudes: 40°N and 70°N . The longitude of the simulations was set to 0°E . In the beginning of each scenario simulation, all SIC ion concentrations were set to zero (i.e., to very different values compared to the “truth”). To enforce similar ionization and atmospheric conditions for the scenarios, SIC used WACCM-D output data as input as follows:

1. WACCM-D data at full hours from longitude 0°E were used in SIC from half- to 15-past of each hour (SIC was run with a 15 min time step). For example, SIC output for 11:30, 11:45, 12:00, and 12:15 UT used WACCM-D output at 12:00 UT.
2. All WACCM-D data profiles were interpolated from pressure levels to the SIC 1 km altitude grid using geometric altitudes calculated from WACCM-D geopotential heights.
3. WACCM-D data used: temperature, N_2O , NO , NO_2 , NO_3 , HNO_3 , N_2O_5 , H_2O , CO_2 , H , H_2 , HCl , Cl , ClO , CH_4 , N_2O , CO , CH_2O , and O . These include the long-lived species and chlorine species which SIC considers as static background only. Note that concentrations of NO_y species are solved by SIC, but in the current study, we set them to WACCM-D values at each time step and all altitudes because of (1) the importance of NO for D-region ionization by Lyman- α radiation and (2) the potentially large discrepancies between the models below 40 km that could lead to differences in the ion composition. Also H and O are solved by SIC, but here we used concentrations from WACCM-D because above 80 km these two species have relatively long chemical lifetimes and are subject to transport in WACCM-D.
4. WACCM-D EUV/soft X-ray ionization rates used: O , O_2 , N_2 , and NO . WACCM-D SPE ionization rates, i.e., C. H. Jackman’s daily values. GCR as in WACCM-D.

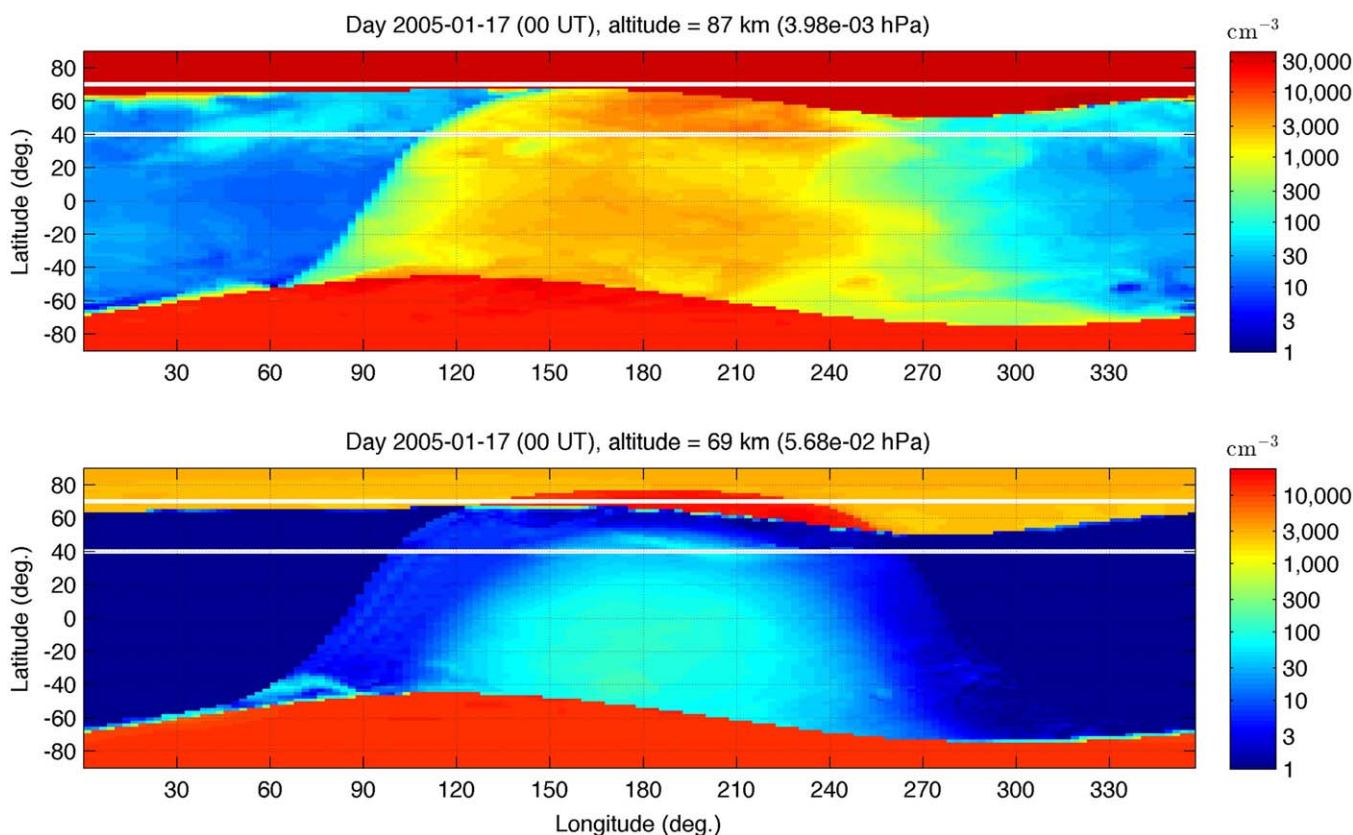


Figure 4. WACCM-D global electron concentration on 17 January 2005, at 00 UT. (top) Altitude = 87 km. (bottom) Altitude = 69 km. The white horizontal lines at latitudes 40°N and 70°N correspond to ionization scenarios SC1 and SC2, respectively.

It is important to note that WACCM-D and SIC are separate models. The neutral species and ionization rates from WACCM-D were used in the SIC calculations (instead of those SIC would calculate) to keep the models as similar as possible in this respect, thus minimizing their effects on the comparison. The differences in ion composition caused by different sets of ions and ion chemistry in WACCM-D and SIC remain and are better assessed with this approach.

5.3. Comparison

In the following (section 6), we present results from WACCM-D and compare the concentrations of species to those from SIC. We concentrate on the D-region ionosphere only, i.e., below 90 km. There are some clear differences between the models at altitudes above, but we did not pursue to discuss or solve these as this is outside the scope of this paper. Comparison is done for full UT hours between 15 and 20 January, i.e., there were altogether 144 temporal comparison points. Note that because of the zero starting values for ions in SIC and the resulting model spin-up, we excluded 14 January from the comparison as it takes about 1 day for SIC to “catch up.” For statistical comparisons of the concentrations, we calculated the following: (a) mean altitude profiles, (b) WACCM-D relative bias ($= 100 \times \text{mean}(\text{WACCM-D} - \text{SIC})/\text{mean}(\text{SIC})$), and (c) standard deviation of the bias. These were calculated separately for daytime and nighttime, to reveal diurnal differences. We begin the comparison with electron concentrations and the sums of positive and negative ions. This is useful for looking at the overall ionospheric behavior. We then proceed to selected groups of ions, concentrating on those that are important when modeling effects of particle precipitation on minor neutral composition. The definitions of the ion groups are given in the Appendix A.

We excluded the sunrise/sunset times from the comparison because the models handle the solar flux scaling of reaction rate coefficients differently. Scaling is needed for a number of ionic reactions that are most important below 80 km and require solar radiation [Verronen *et al.*, 2006b]: positive ion photodissociation (PPI), photodetachment of electrons from negative ions (EPN), and negative ion photodissociation (PNI) reactions. In WACCM-D, the scaling is simply an on/off (or 1/0) switch between day and night, the daytime/

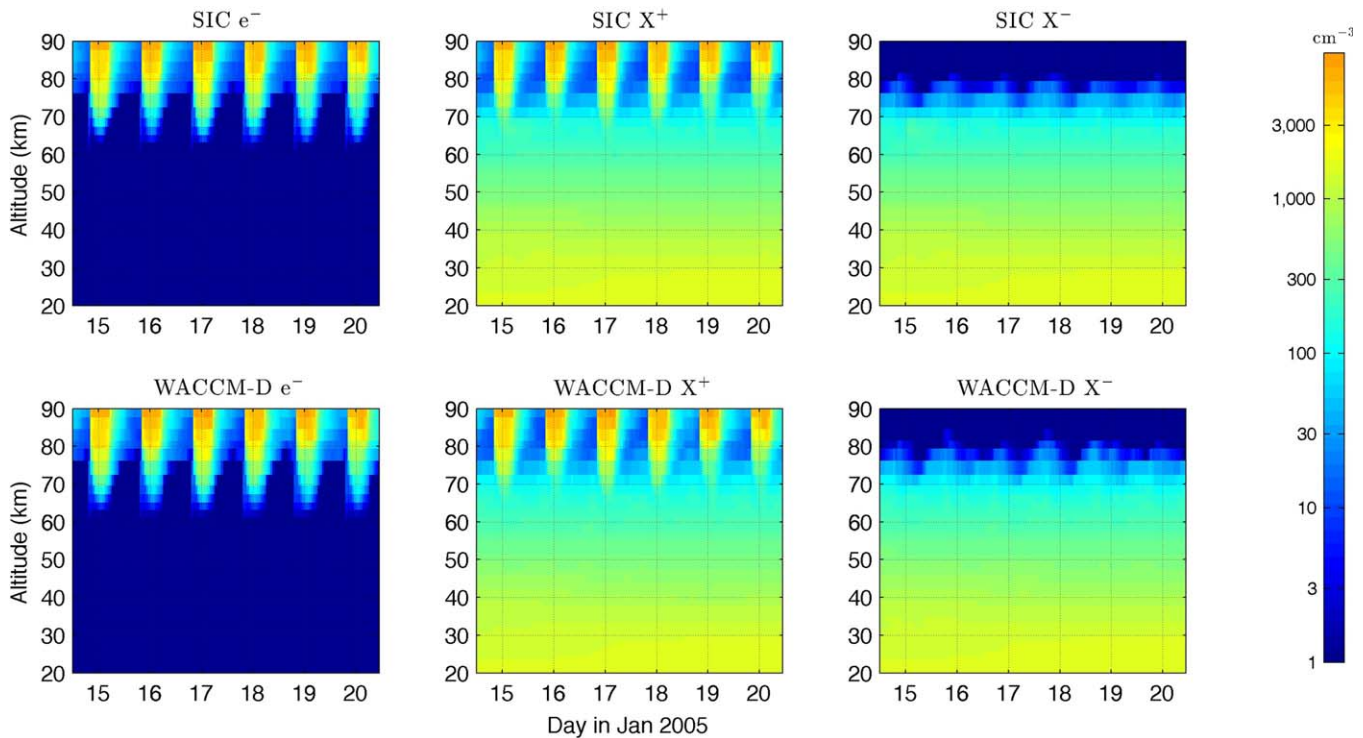


Figure 5. Scenario SC1. (left) Electron, (middle) positive ion, and (right) negative ion concentration in cm^{-3} . (top row) SIC; (bottom row) WACCM-D. x axis tick marks are at noon each day.

nighttime value being applied at solar zenith angles smaller/larger than 97° . In SIC, the scaling is done based on the calculated amount of solar radiation available at each altitude, relative to midlatitude noon amount, which below 80 km leads to a smoother transition between day and night compared to WACCM-D.

Another notable difference between the models is the transport (advection) in WACCM-D but not in SIC (1-D SIC only represents vertical diffusion). All species are transported in WACCM-D, including the ions. The ions in general have relatively short chemical lifetimes, compared to dynamical lifetimes, so transport should not have much direct influence on the ions or the model-model comparison. In fact, in later versions of WACCM/WACCM-D, which will have the ability to switch off advection for selected species, the computing time could be reduced by switching off the transport for the ions. Note, however, that although the ions are not much affected by transport, an indirect effect could be important through transport of neutral species that participate in ionic reactions.

6. Results and Discussion

Figure 5 shows the electron concentration and the sums of positive and negative ions for Scenario SC1 (described in Table 3). Overall, the WACCM-D results are very similar to those from SIC, and important features of the lower ionosphere are clear and well presented: (1) diurnal variation of electron concentration due to EUV ionization above about 65 km, and (2) gradual transition from electrons to negative ions with decreasing altitude, and (3) domination of negative ions over electrons below about 65 km and 80 km at day and night, respectively. Because the GCR ionization does not have diurnal variability, the lower altitudes show more or less constant concentrations throughout the modeling period. As expected, the negative ion concentration is very small above about 80 km because electron attachment to neutral species, causing production of initial negative ions, depends on total atmospheric density and thus its rate slows down with increasing altitude. The mean concentration profiles from SIC and WACCM-D, together with WACCM-D bias, are presented for daytime in Figure 6. The daytime mean profiles are very close to each other, and the bias is generally within $\pm 10\%$ and in many cases not more than just a few percent. In contrast, there is a larger

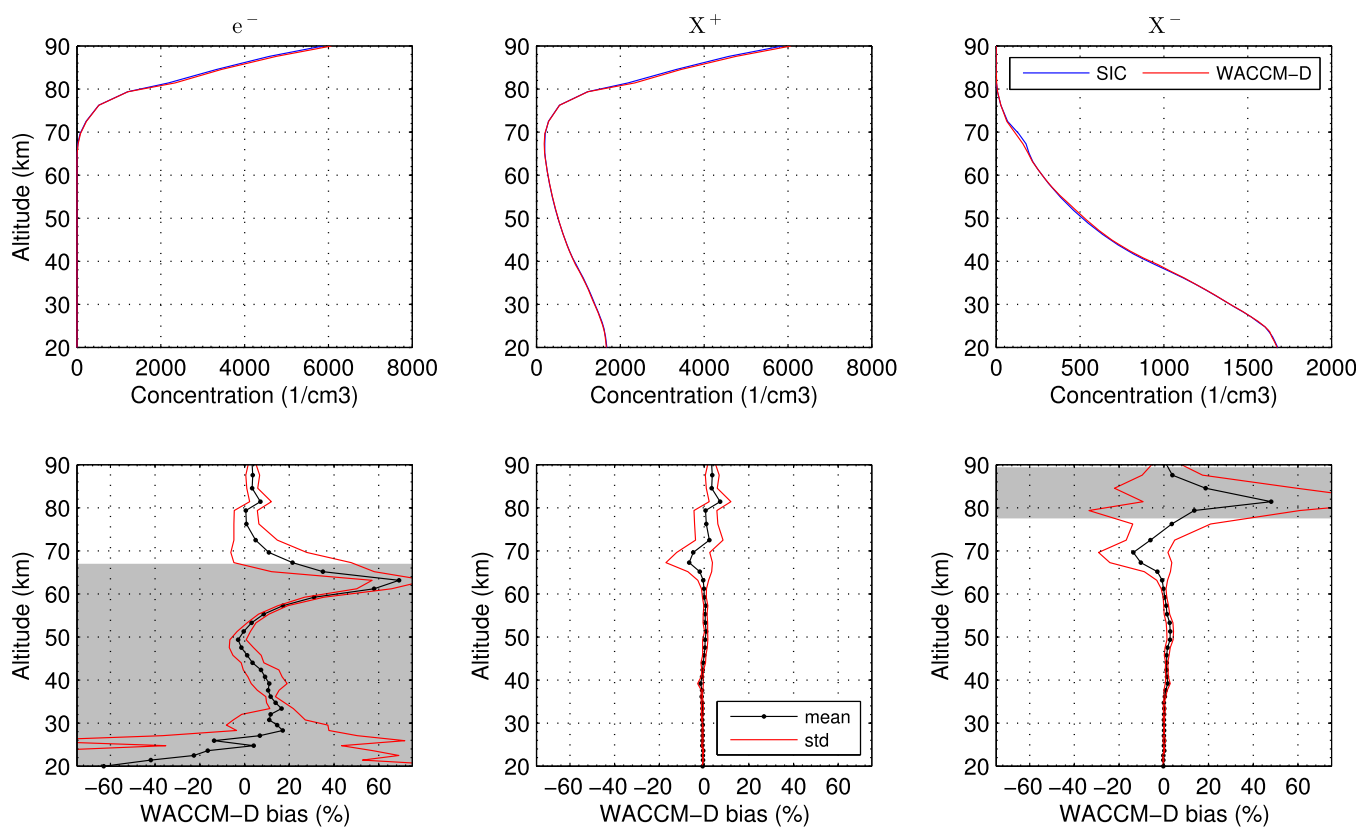


Figure 6. Scenario SC1. (top) (left) Average daytime (SZA = 60–75°) electron, (middle) positive ion, and (right) negative ion concentrations. (bottom) Relative mean WACCM-D bias (black line) and its standard deviation (red line). Altitudes where absolute concentration of the species is less than 5% of the total negative charge have a gray shading.

bias of electrons and negative ions below 40 km and above 75 km, respectively. However, these are altitude regions where the proportion of electrons and ions, respectively, is small relative to the total negative charge (<5%). In absolute concentrations (not shown), the differences seen at these altitudes are small. Electron concentration has a positive bias of about 70% in a narrow region around 65 km, coinciding with a strong altitude gradient in photoionization and electron concentration as seen in Figures 3 and 5, so the differences in altitude resolution between the models and related uncertainties are likely contributing to the bias.

The comparison is nearly as good for nighttime, as shown in Figure 7, except that above 80 km the electron and positive ion bias is about 40–70%. Looking again at these species in Figure 5, the diurnal variability at the upper altitudes is very similar in the two models. Compared to daytime, absence of solar EUV radiation leads to decrease in ionic concentrations by several orders of magnitude at night. However, the relaxation to nighttime values seems to be faster in SIC than in WACCM-D so that the SIC concentrations are clearly smaller just before sunrise. The gradual increase in the WACCM-D bias is reflected in the standard deviation, i.e., it is much larger than in the daytime (Figure 6). Since the ionization rate (i.e., production of electron-ion pairs) is the same in the two models, it seems that the differences could be related to the recombination (causing the loss electrons and ions) which is simplified in WACCM-D. However, as shown in Figure 4 (top), the WACCM-D electron (and ion, not shown) concentration also reflects the turbulent dynamics especially around sunset (210°–330° longitude), which seems to delay the relaxation. Obviously, such dynamics cannot be represented in 1-D SIC, which likely explains why it shows a more rapid relaxation for SC1 (40°N).

Figure 8 shows the electron concentration and the sums of positive and negative ions for Scenario SC2. Compared to SC1 (Figure 5), the SPE ionization enhances the electron and ion concentrations by several orders of magnitude. Due to the strong forcing, the diurnal variation between high-electron (daytime) and high-negative-ion (nighttime) concentration is seen more clearly at 50–80 km. Again, the concentrations from WACCM-D are comparable to those from SIC, both the altitude and temporal variations are generally

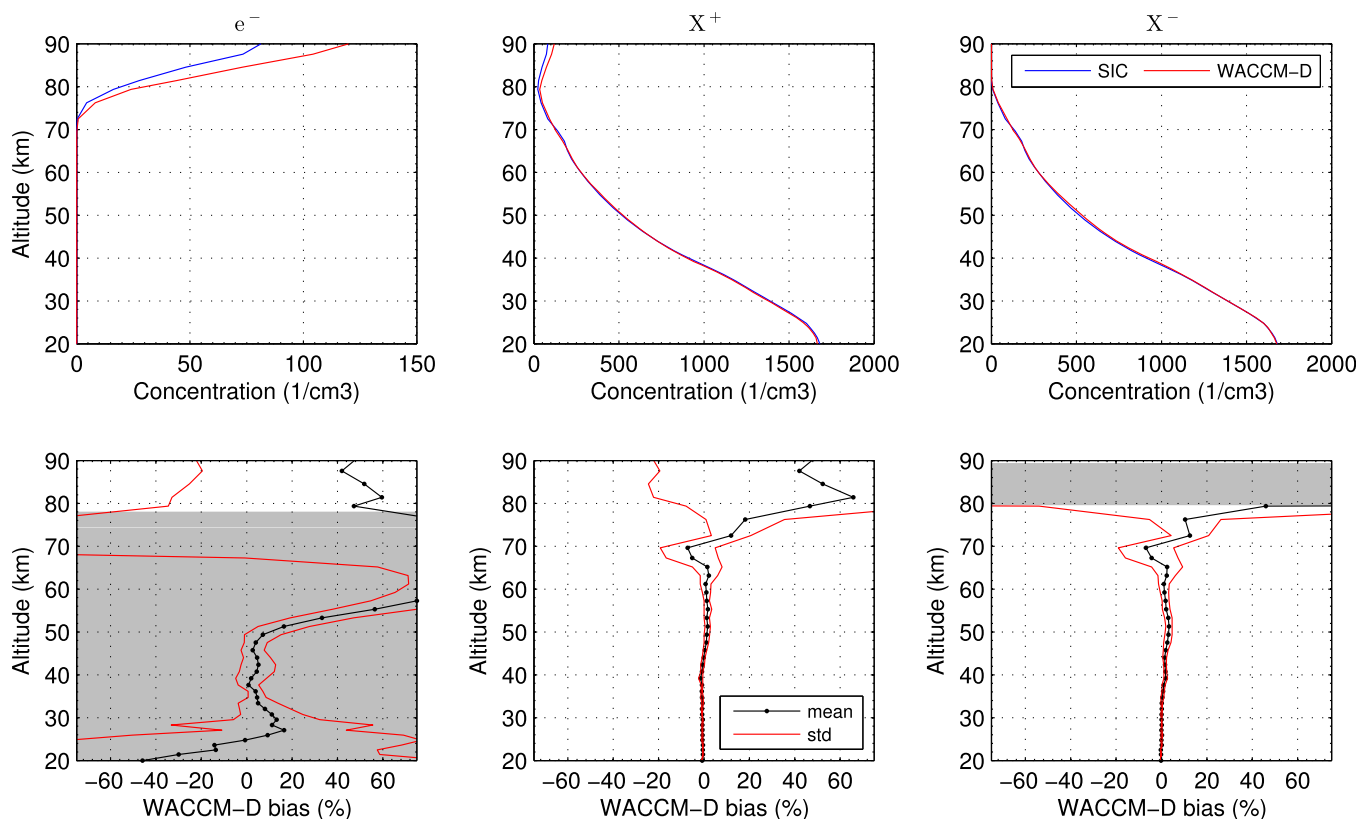


Figure 7. Scenario SC1. (top) (left) Average nighttime (SZA = 101–131°) electron, (middle) positive ion, and (right) negative ion concentrations. (bottom) Relative mean WACCM-D bias (black line) and its standard deviation (red line). Altitudes where absolute concentration of the species is less than 5% of the total negative charge have a gray shading.

well captured. For these species, nighttime WACCM-D bias for SC2 (not shown) is generally smaller than for SC1 (Figure 7), and especially so at altitudes above 75 km where it is within 20%.

Since the aim of WACCM-D development is to represent the changes in neutral species during EPP, it is interesting to compare the groups of ions that are important in that context. Figure 9 shows the SC2 sum of concentration for three groups: $H^+(H_2O)_n$, $NO_3^-(HNO_3)_n$, and $Cl^-(X)$ (for ion group definitions, see the Appendix A1). The first two are important because their formation and recombination is part of many reaction sequences that produce HO_x from water vapor and nitric acid from NO_x [Verronen and Lehmann, 2013]. Comparison with total ion sums (Figure 8) indicates that $H^+(H_2O)_n$ and $NO_3^-(HNO_3)_n$ are a substantial part of the total charge below 80 km, while $Cl^-(X)$ is abundant especially at 40–65 km during daytime. The concentration of $H^+(H_2O)_n$ is small above 80 km because the rapidly declining amount of H_2O restricts the formation of water cluster ions. The concentrations and thus the proportions of these groups are quite similar in the two models. However, there are also small differences. For example, the sunset/sunrise transitions are sharper in WACCM-D due to differences in the solar flux scaling of some ionic reactions (e.g., photodetachment reactions). Overall, there are more differences in these ion groups than there is in the total ion sums. This is natural because the overall charge content is basically the balance between ionization and recombination, while the ion composition is also affected by the different sets of ions and reactions in the models. Figure 10 shows a nighttime statistical comparison of the same ion groups. For $Cl^-(X)$, the altitude behavior of the mean profiles is similar but there are large differences in absolute concentrations. The WACCM-D bias is generally within $\pm 40\%$ (although significantly larger around 35–40 km), despite the $Cl^-(X)$ concentration being less than 5% of the total negative charge at most altitudes. Note that during periods when $Cl^-(X)$ is more abundant the differences become smaller below 65 km (Figure 9, right), and similar improvement is seen for SC1 as well (not shown). For $H^+(H_2O)_n$ and $NO_3^-(HNO_3)_n$, the agreement is very good below 70 km. At 70–80 km, there is a positive WACCM-D bias reaching 50% and 40% at 75 km, respectively, coinciding with strong gradients in their concentrations. Nevertheless, the altitude behavior of the mean profiles of these ions is clearly very similar.

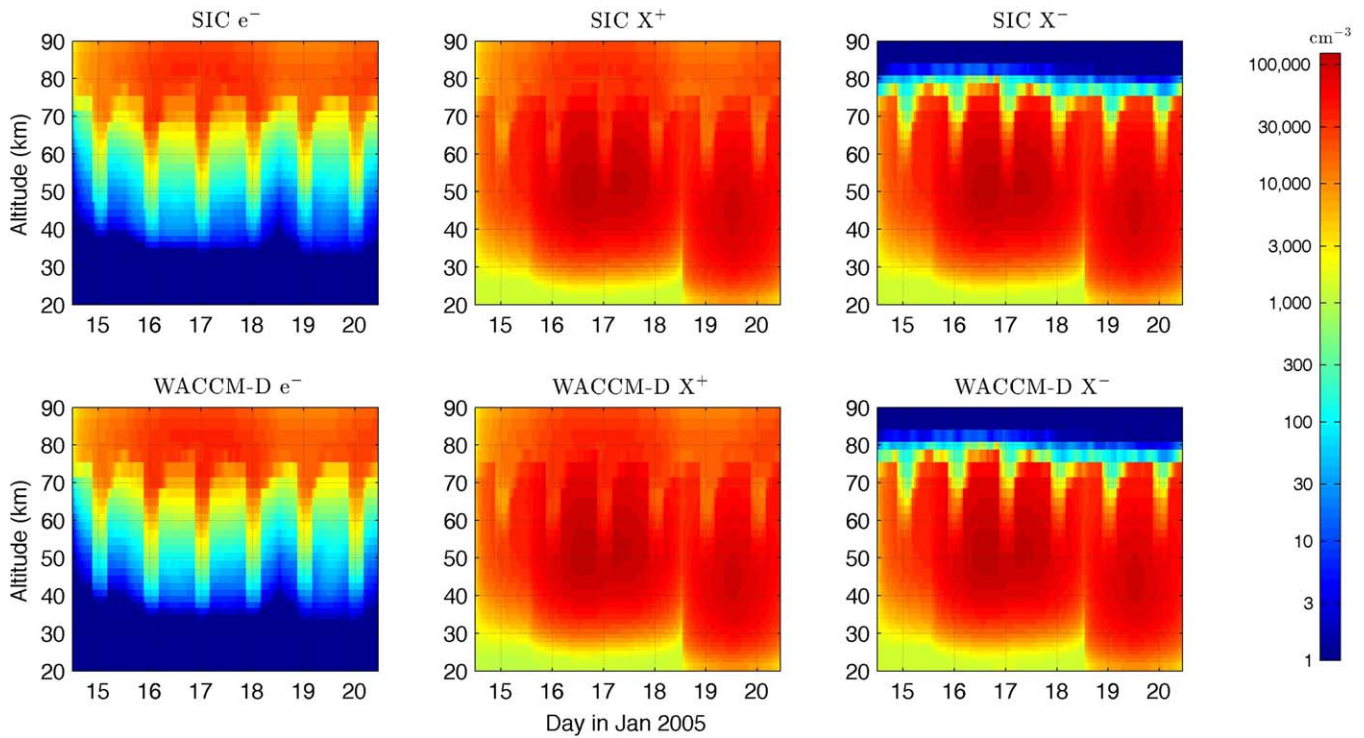


Figure 8. Scenario SC2. (left) Electron, (middle) positive ion, and (right) negative ion concentration in cm^{-3} . (top row) SIC; (bottom row) WACCM-D. x axis tick marks are at noon each day.

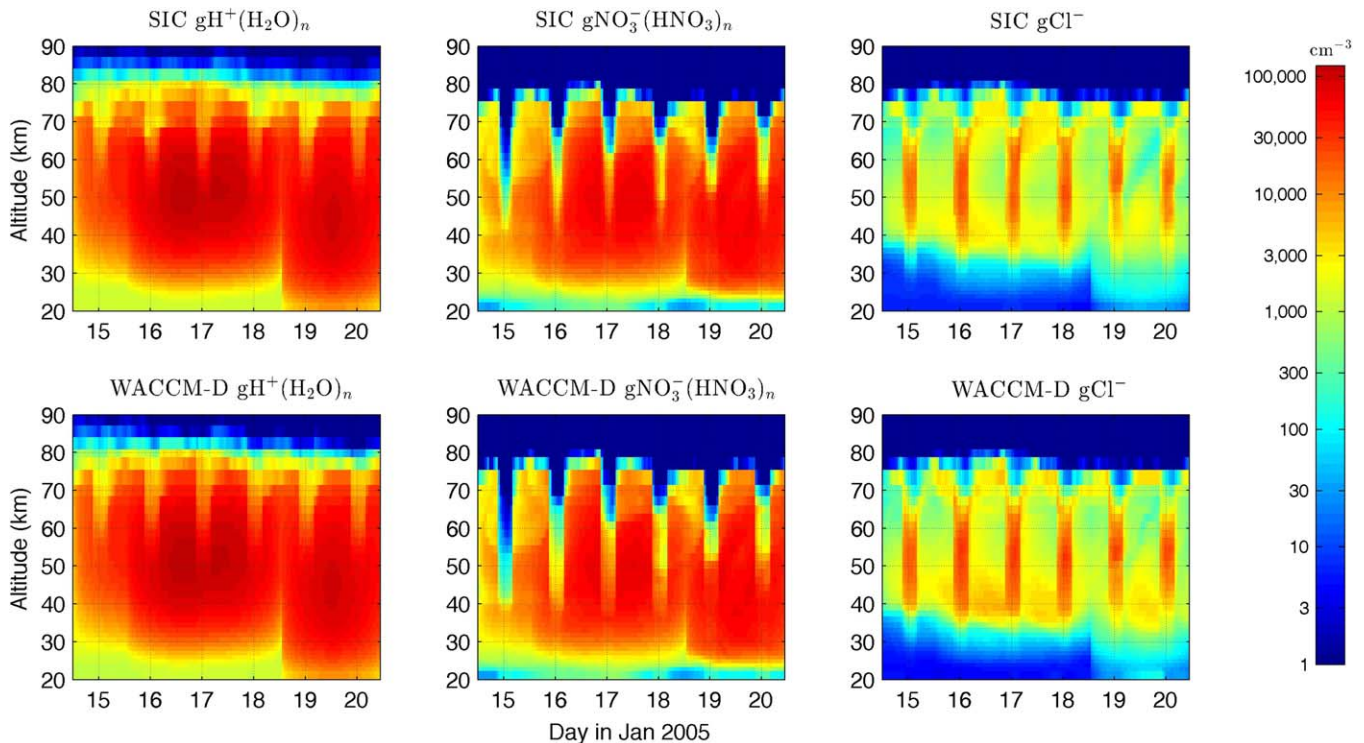


Figure 9. Scenario SC2. Sum of concentration in cm^{-3} for selected ion groups. (top row) SIC; (bottom row) WACCM-D. x axis tick marks are at noon each day.

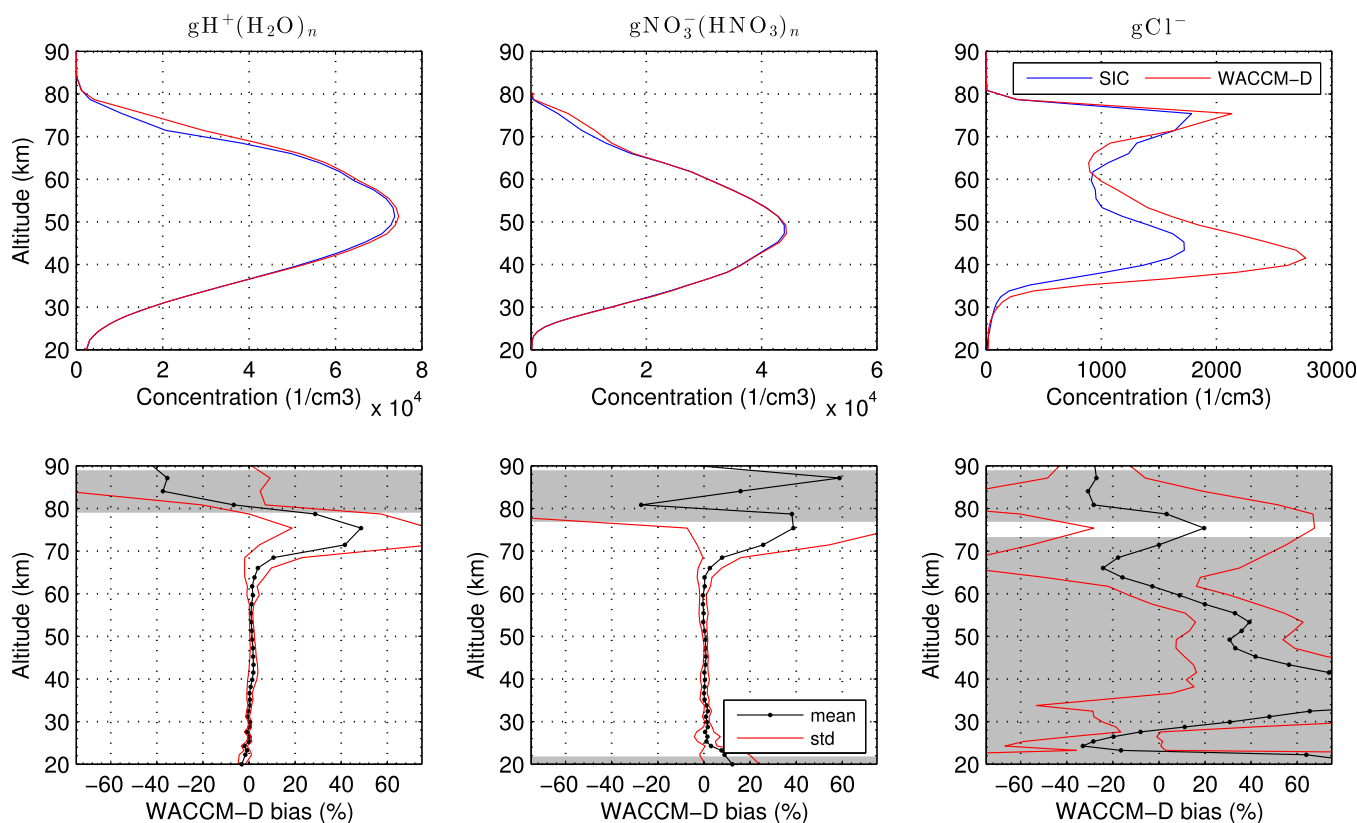


Figure 10. Scenario SC2. (top) Average nighttime (SZA = 101–131°) concentrations of selected ion groups. (bottom) Relative mean WACCM-D bias (black line) and its standard deviation (red line). Altitudes where absolute concentration of the group is less than 5% of the total negative charge have a gray shading.

7. Conclusions

We have presented WACCM-D, a variation of the Whole Atmosphere Community Climate Model including a selected set of D-region ion chemistry. The purpose of WACCM-D is to better reproduce the neutral atmospheric effects caused by EPP in the polar regions.

We have shown that WACCM-D produces the main characteristics of the D-region ionosphere, as well as the overall proportion of different ion groups. Comparison to the SIC model, which includes a much more extensive set of ion chemistry, indicates good agreement between the models. Below 70 km, WACCM-D bias is generally within ±10% or less, except in cases where the ion group in question has a relatively small concentration (compared to the total charge content) at certain altitudes. At 70–90 km, when strong altitude gradients in ionization rates and ion concentrations are seen, the bias is typically larger and can reach several tens of percent for some ion groups (up to 50%). At these altitudes, turbulent dynamics in the global WACCM-D model seem to affect the ion concentrations indirectly (through neutral species participating in ionic reactions) especially around sunset times, which could contribute to the nighttime bias in some cases because these effects cannot be reproduced in 1-D SIC.

The comparison between WACCM-D and SIC is not perfect, nor should it be because the models are by nature very different (3-D WACCM-D compared to 1-D SIC) and there are significant differences in ion chemistry. For example, there is a much larger ion chemistry scheme in SIC and solar flux scaling of the photodetachment reactions is handled differently. However, based on the good agreement overall and the fact that part of the differences are caused by different model setups (e.g., altitude resolution, transport processes), WACCM-D now provides a state-of-the-art representation of D-region ion chemistry globally in 3-D and is therefore expected to improve the EPP modeling considerably. In the companion paper (Andersson et al., submitted manuscript, 2016), this is demonstrated in the case of the SPE of January 2005.

Appendix A: WACCM-D Ions and Ionic Reactions

In this Appendix, we list the ions, ion groups, reactions, and rate coefficients used in WACCM-D. In some cases, comparison to the SIC model is made using a color code:

Blue	In SIC	In WACCM (and WACCM-D)
White (i.e., no color)	In SIC	In WACCM-D
Gray	In SIC	Not in WACCM-D
Red	Not in SIC	In WACCM (and WACCM-D)

A1. Definition of Ion Groups

A1.1. Definition of Positive Ion Groups

Ion Group				
gNp	gOp	gNOp	gHp	
N^+	O^+	NO^+	$H_3O^+(OH)$	
N_2^+	O_2^+	$NO^+(N_2)$	$H^+(H_2O)$	
	O_4^+	$NO^+(CO_2)$	$H^+(H_2O)_2$	
	$O_2^+(H_2O)$	$NO^+(H_2O)$	$H^+(H_2O)_3$	
	$O_2^+(N_2)$	$NO^+(H_2O)_2$	$H^+(H_2O)_4$	
	$O_2^+(CO_2)$	$NO^+(H_2O)_3$	$H^+(H_2O)_5$	
	$O_2^+(H_2O)(N_2)$	$NO^+(H_2O)(N_2)$	$H^+(H_2O)_6$	
	$O_2^+(H_2O)(CO_2)$	$NO^+(H_2O)(CO_2)$	$H^+(H_2O)_7$	
	$O_2^+(H_2O)_2$	$NO^+(H_2O)_2(N_2)$	$H^+(H_2O)_8$	
		$NO^+(H_2O)_2(CO_2)$	$H^+(H_2O)_2(CO_2)$	
			$H^+(H_2O)_2(N_2)$	
			$H^+(H_2O)(CO_2)$	
			$H^+(H_2O)(N_2)$	
			$H_3O^+(OH)(H_2O)$	
			$H_3O^+(OH)(CO_2)$	
			$H^+(H_2O)(HNO_3)$	
			$H^+(H_2O)_2(HNO_3)$	
			$H^+(H_2O)_3(HNO_3)$	
			$H^+(H_2O)_4(HNO_3)$	
			$H^+(H_2O)_5(HNO_3)$	

A1.2. Definition of Negative Ion Groups

Ion Groups				
gOHm	gCOM	gClm	gOm	gNOM
OH^-	CO_3^-	Cl^-	O^-	NO_2^-
HCO_3^-	CO_4^-	$Cl^-(H_2O)$	O_2^-	NO_3^-
$OH^-(H_2O)$	$CO_3^-(H_2O)$	ClO^-	O_3^-	$NO_3^- (*)$
	$CO_3^-(H_2O)_2$	$Cl^-(CO_2)$	O_4^-	$NO_3^-(H_2O)$
		$Cl^-(HCl)$	$O_2^-(H_2O)$	$NO_2^-(H_2O)$
			$O_3^-(H_2O)$	$NO_3^-(H_2O)_2$
			$O^-(H_2O)$	$NO_3^-(HNO_3)$
			$O_2^-(H_2O)_2$	$NO_3^-(HNO_3)_2$
				$NO_3^-(HCl)$

A2. Reactions and Rate Coefficients

A2.1. Positive Ion Reactions (PIR)

Nr	Reactants	Products	Reaction Rate Coefficient	Source
1	$O^+ + O_2$	$O_2^+ + O$	2.1×10^{-11a}	Roble [1995]
2	$O^+ + N_2$	$NO^+ + N$	1.02×10^{-12a}	Roble [1995]
3	$O^+ + CO_2$	$O_2^+ + CO$	9.0×10^{-10}	Roble [1995]
4	$O_2^+ + NO$	$NO^+ + O_2$	4.4×10^{-10}	Roble [1995]
5	$O_2^+ + N_2$	$NO^+ + NO$	5.0×10^{-16}	Roble [1995]
6	$O_2^+ + O_2 + M$	$O_4^+ + M$	$4.0 \times 10^{-30} \times (300/T)^{2.93}$	Böhlinger and Arnold [1982]
7	$O_2^+ + H_2O + M$	$O_2^+(H_2O) + M$	2.8×10^{-28}	Albritton [1978]
8	$O_2^+ + N$	$NO^+ + O$	1.0×10^{-10}	Roble [1995]
9	$O_4^+ + O_2(^1\Delta_g)$	$O_2^+ + 2O_2$	1.5×10^{-10}	Fehsenfeld et al. [1971]
10	$O_4^+ + H_2O$	$O_2^+(H_2O) + O_2$	1.7×10^{-9}	Rakshit and Warneck [1980]
11	$O_4^+ + O$	$O_2^+ + O_3$	3.0×10^{-10}	Albritton [1978]
12	$N^+ + O_2$	$NO^+ + O$	2.0×10^{-10}	Roble [1995]
13	$N^+ + O_2$	$O_2^+ + N$	4.0×10^{-10}	Roble [1995]
14	$N^+ + O$	$O^+ + N$	1.0×10^{-12}	Roble [1995]
15	$N_2^+ + O$	$NO^+ + N(^2D)$	$1.4 \times 10^{-10} \times (300/T)^{0.44}$	Roble [1995]
16	$N_2^+ + O$	$O^+ + N_2$	1.0×10^{-11a}	Roble [1995]
17	$N_2^+ + O_2$	$O_2^+ + N_2$	6.0×10^{-11}	Roble [1995]
18	$NO^+ + N_2 + M$	$NO^+(N_2) + M$	$3.0 \times 10^{-31} \times (300/T)^{4.3}$	Dheandhanoo and Johnsen [1983]
19	$NO^+ + CO_2 + M$	$NO^+(CO_2) + M$	$1.4 \times 10^{-29} \times (300/T)^4$	Dheandhanoo and Johnsen [1983]
20	$NO^+ + H_2O + M$	$NO^+(H_2O) + M$	$1.35 \times 10^{-28} \times (300/T)^{2.83}$	Eyet et al. [2011]
21	$NO^+(N_2) + CO_2$	$NO^+(CO_2) + N_2$	1.0×10^{-9}	Thomas [1976]
22	$NO^+(N_2) + H_2O$	$NO^+(H_2O) + N_2$	1.0×10^{-9}	Reid [1977]
23	$NO^+(N_2) + M$	$NO^+ + N_2 + M$	$1.5 \times 10^{-8} \times (300/T)^{4.3} \times e^{-2093/T}$	Dheandhanoo and Johnsen [1983]
24	$NO^+(CO_2) + H_2O$	$NO^+(H_2O) + CO_2$	1.0×10^{-9}	Reid [1977]
25	$NO^+(CO_2) + M$	$NO^+ + CO_2 + M$	$3.4 \times 10^{-7} \times (300/T)^5 \times e^{-3872/T}$	Pavlov [2013]
26	$NO^+(H_2O) + HO_2$	$H^+(H_2O) + NO_3$	0.5×10^{-9}	Fehsenfeld et al. [1975]
27	$NO^+(H_2O) + OH$	$H^+(H_2O) + NO_2$	1.0×10^{-10}	Albritton [1978]
28	$NO^+(H_2O) + H$	$H^+(H_2O) + NO$	7.0×10^{-12}	Fehsenfeld et al. [1975]
29	$NO^+(H_2O) + H_2O + M$	$NO^+(H_2O)_2 + M$	$1.0 \times 10^{-27} \times (308/T)^{4.7}$	Reid [1977]
30	$NO^+(H_2O)_2 + H_2O + M$	$NO^+(H_2O)_3 + M$	$1.0 \times 10^{-27} \times (308/T)^{4.7}$	Reid [1977]
31	$NO^+(H_2O)_3 + H_2O$	$H^+(H_2O)_3 + HNO_2$	7.0×10^{-11}	Reid [1977]
32	$O_2^+(H_2O) + H_2O$	$H_3O^+(OH) + O_2$	9.0×10^{-10}	Rakshit and Warneck [1980]
33	$O_2^+(H_2O) + H_2O$	$H^+(H_2O) + OH + O_2$	2.4×10^{-10}	Albritton [1978]
34	$H_3O^+(OH) + H_2O$	$H^+(H_2O)_2 + OH$	2.0×10^{-9}	Albritton [1978]
35	$H^+(H_2O) + H_2O + M$	$H^+(H_2O)_2 + M$	$4.6 \times 10^{-27} \times (300/T)^4$	Lau et al. [1982]
36	$H^+(H_2O)_2 + M$	$H^+(H_2O) + H_2O + M$	$2.5 \times 10^{-2} \times (300/T)^5 \times e^{-15900/T}$	Lau et al. [1982]
37	$H^+(H_2O)_2 + H_2O + M$	$H^+(H_2O)_3 + M$	$2.3 \times 10^{-27} \times (300/T)^{7.5}$	Lau et al. [1982]
38	$H^+(H_2O)_3 + M$	$H^+(H_2O)_2 + H_2O + M$	$2.6 \times 10^{-3} \times (300/T)^{8.5} \times e^{-10272/T}$	Pavlov [2013]
39	$H^+(H_2O)_3 + H_2O + M$	$H^+(H_2O)_4 + M$	$3.6 \times 10^{-27} \times (300/T)^{8.1}$	Lau et al. [1982]
40	$H^+(H_2O)_4 + M$	$H^+(H_2O)_3 + H_2O + M$	$1.5 \times 10^{-1} \times (300/T)^{9.1} \times e^{-9000/T}$	Lau et al. [1982]
41	$H^+(H_2O)_4 + H_2O + M$	$H^+(H_2O)_5 + M$	$4.6 \times 10^{-28} \times (300/T)^{14}$	Lau et al. [1982]
42	$H^+(H_2O)_5 + M$	$H^+(H_2O)_4 + H_2O + M$	$1.7 \times 10^{-3} \times (300/T)^{15} \times e^{-6400/T}$	Lau et al. [1982]
43	$H^+(H_2O)_4 + N_2O_5$	$H^+(H_2O)_3(HNO_3) + HNO_3$	4.0×10^{-12}	Böhlinger et al. [1983]
44	$H^+(H_2O)_5 + N_2O_5$	$H^+(H_2O)_4(HNO_3) + HNO_3$	7.0×10^{-12}	Böhlinger et al. [1983]
45	$H^+(H_2O)_3(HNO_3) + H_2O$	$H^+(H_2O)_4 + HNO_3$	1.0×10^{-9}	Böhlinger et al. [1983]
46	$H^+(H_2O)_4(HNO_3) + H_2O$	$H^+(H_2O)_5 + HNO_3$	1.0×10^{-9}	Böhlinger et al. [1983]

^aApproximately; see the reference for details.

A2.2. Recombination of Positive Ions With Electrons (RPE)

Nr	Reactants	Products	Reaction Rate Coefficient	Source
1	$O_2^+ + e$	$1.15O + 0.85O(^1D)$	$2.7 \times 10^{-7} \times (300/T)^{0.7}$	Roble [1995]
2	$O_4^+ + e$	$2O_2$	$4.2 \times 10^{-6} \times (300/T)^{0.5}$	Johnsen [1987]
3	$N_2^+ + e$	$1.1N + 0.9N(^2D)$	$1.8 \times 10^{-7} \times (300/T)^{0.39}$	Roble [1995]
4	$NO^+ + e$	$0.2N + 0.8N(^2D) + O$	$4.2 \times 10^{-7} \times (300/T)^{0.85}$	Roble [1995]
5	$NO^+(N_2) + e$	$NO + N_2$	$1.4 \times 10^{-6} \times (300/T)^{0.4}$	Johnsen [1987]
6	$NO^+(CO_2) + e$	$NO + CO_2$	1.5×10^{-6}	Swider and Narcisi [1975]
7	$NO^+(H_2O) + e$	$NO + H_2O$	1.5×10^{-6}	Swider and Narcisi [1983]
8	$NO^+(H_2O)_2 + e$	$NO + 2H_2O$	2.0×10^{-6}	Swider and Narcisi [1983]
9	$NO^+(H_2O)_3 + e$	$NO + 3H_2O$	2.0×10^{-6}	Swider and Narcisi [1983]

(continued)

Table (continued)

Nr	Reactants	Products	Reaction Rate Coefficient	Source
10	$O_2^+(H_2O) + e$	$\rightarrow O_2 + H_2O$	2.0×10^{-6}	Swider and Narcisi [1983]
11	$H_3O^+(OH) + e$	$\rightarrow OH + H + H_2O$	1.5×10^{-6}	Swider and Narcisi [1983]
12	$H^+(H_2O) + e$	$\rightarrow H + H_2O$	$6.3 \times 10^{-7} \times (300/T)^{0.5}$	McGowan and Mitchell [1984]
13	$H^+(H_2O)_2 + e$	$\rightarrow H + 2H_2O$	$2.5 \times 10^{-6} \times (300/T)^{0.1}$	Johnsen [1987]
14	$H^+(H_2O)_3 + e$	$\rightarrow H + 3H_2O$	$2.48 \times 10^{-6} \times (300/T)^{0.76}$	Öjekull et al. [2007]
15	$H^+(H_2O)_4 + e$	$\rightarrow H + 4H_2O$	3.6×10^{-6}	Johnsen [1987]
16	$H^+(H_2O)_5 + e$	$\rightarrow H + 5H_2O$	5.0×10^{-6}	Johnsen [1987]

A2.3. Positive Ion Photodissociation (PPI)

Nr	Reactants	Products	Reaction Rate Coefficient	Source
1	$O_2^+(H_2O) + h\nu$	$\rightarrow O_2^+ + H_2O$	0.42	Smith et al. [1978]

A2.4. Electron Attachment on Neutrals (EAN)

Nr	Reactants	Products	Reaction Rate Coefficient	Source
1	$O_2 + N_2 + e$	$\rightarrow O_2^- + N_2$	$1.0 \times 10^{-31} \times (300/T) \times e^{-600/T}$	Phelps [1969]
2	$O_3 + e$	$\rightarrow O^- + O_2$	$9.1 \times 10^{-12} \times (300/T)^{-1.46}$	Stelman et al. [1972]
3	$2O_2 + e$	$\rightarrow O_2^- + O_2$	$4.0 \times 10^{-30} \times e^{-193/T}$	Truby [1972]

A2.5. Negative Ion Reactions (NIR)

Nr	Reactants	Products	Reaction Rate Coefficient	Source
1	$O^- + O_3$	$\rightarrow O_3^- + O$	8.0×10^{-10}	Ikezoe et al. [1987]
2	$O^- + 2O_2$	$\rightarrow O_3^- + O_2$	1.4×10^{-30}	Payzant and Kebarle [1972]
3	$O^- + H_2O$	$\rightarrow OH^- + OH$	6.0×10^{-13}	Albritton [1978]
4	$O^- + NO_2$	$\rightarrow NO_2^- + O$	1.0×10^{-9}	Ikezoe et al. [1987]
5	$O^- + CO_2 + M$	$\rightarrow CO_3^- + M$	2.0×10^{-28}	Albritton [1978]
6	$O^- + H_2$	$\rightarrow OH^- + H$	3.2×10^{-11}	Brasseur and Baets [1986]
7	$O^- + HCl$	$\rightarrow Cl^- + OH$	2.7×10^{-9}	Turco [1977]
8	$O^- + Cl$	$\rightarrow Cl^- + O$	1.0×10^{-10}	Turco [1977]
9	$O^- + ClO$	$\rightarrow Cl^- + O_2$	1.0×10^{-10}	Turco [1977]
10	$O^- + HNO_3$	$\rightarrow NO_3^- + OH$	3.6×10^{-9}	Huey [1996]
11	$O_2^- + O$	$\rightarrow O^- + O_2$	1.5×10^{-10}	Ikezoe et al. [1987]
12	$O_2^- + O_3$	$\rightarrow O_3^- + O_2$	7.8×10^{-10}	Fehsenfeld and Ferguson [1974]
13	$O_2^- + CO_2 + O_2$	$\rightarrow CO_4^- + O_2$	4.7×10^{-29}	Ikezoe et al. [1987]
14	$O_2^- + NO_2$	$\rightarrow NO_2^- + O_2$	7.0×10^{-10}	Ikezoe et al. [1987]
15	$O_2^- + O_2 + M$	$\rightarrow O_4^- + M$	3.4×10^{-31}	Albritton [1978]
16	$O_2^- + HCl$	$\rightarrow Cl^- + HO_2$	2.0×10^{-9}	Turco [1977]
17	$O_2^- + Cl$	$\rightarrow Cl^- + O_2$	1.0×10^{-10}	Turco [1977]
18	$O_2^- + ClO$	$\rightarrow ClO^- + O_2$	1.0×10^{-10}	Turco [1977]
19	$O_2^- + HNO_3$	$\rightarrow NO_3^- + HO_2$	2.9×10^{-9}	Huey [1996]
20	$O_3^- + O$	$\rightarrow O_2^- + O_2$	2.5×10^{-10}	Ikezoe et al. [1987]
21	$O_3^- + H$	$\rightarrow OH^- + O_2$	8.4×10^{-10}	Ikezoe et al. [1987]
22	$O_3^- + CO_2$	$\rightarrow CO_3^- + O_2$	5.5×10^{-10}	Ikezoe et al. [1987]
23	$O_3^- + NO$	$\rightarrow NO_3^- + O$	$1.05 \times 10^{-12} \times (300/T)^{2.15}$	Arnold et al. [1995]
24	$O_3^- + NO_2$	$\rightarrow NO_3^- + O_2$	$2.50 \times 10^{-11} \times (300/T)^{0.79}$	Arnold et al. [1995]
25	$O_3^- + NO_2$	$\rightarrow NO_2^- + O$	$7.5 \times 10^{-11} \times (300/T)^{0.79}$	Arnold et al. [1995]
26	$O_3^- + NO$	$\rightarrow NO_2^- + O_2$	$1.05 \times 10^{-12} \times (300/T)^{2.15}$	Arnold et al. [1995]
27	$O_4^- + O$	$\rightarrow O_3^- + O_2$	4.0×10^{-10}	Ikezoe et al. [1987]
28	$O_4^- + CO_2$	$\rightarrow CO_4^- + O_2$	4.3×10^{-10}	Ikezoe et al. [1987]
29	$OH^- + O_3$	$\rightarrow O_3^- + OH$	9.0×10^{-10}	Ikezoe et al. [1987]
30	$OH^- + NO_2$	$\rightarrow NO_2^- + OH$	1.1×10^{-9}	Ikezoe et al. [1987]
31	$OH^- + CO_2 + M$	$\rightarrow HCO_3^- + M$	7.6×10^{-28}	Ikezoe et al. [1987]
32	$OH^- + HCl$	$\rightarrow Cl^- + H_2O$	1.0×10^{-9}	Turco [1977]

(continued)

Table (continued)

33	$\text{OH}^- + \text{Cl}$	\rightarrow	$\text{Cl}^- + \text{OH}$	1.0×10^{-10}	Turco [1977]
34	$\text{OH}^- + \text{ClO}$	\rightarrow	$\text{ClO}^- + \text{OH}$	1.0×10^{-10}	Turco [1977]
35	$\text{CO}_3^- + \text{O}$	\rightarrow	$\text{O}_2^- + \text{CO}_2$	1.1×10^{-10}	Thomas and Bowman [1985]
36	$\text{CO}_3^- + \text{O}_2$	\rightarrow	$\text{O}_3^- + \text{CO}_2$	6.0×10^{-15}	Albritton [1978]
37	$\text{CO}_3^- + \text{H}$	\rightarrow	$\text{OH}^- + \text{CO}_2$	1.7×10^{-10}	Ikezoe et al. [1987]
38	$\text{CO}_3^- + \text{NO}$	\rightarrow	$\text{NO}_2^- + \text{CO}_2$	$1.3 \times 10^{-11} \times (300/T)^{1.64}$	Arnold et al. [1995]
39	$\text{CO}_3^- + \text{NO}_2$	\rightarrow	$\text{NO}_3^- + \text{CO}_2$	$3.3 \times 10^{-11} \times (300/T)^{2.38}$	Arnold et al. [1995]
40	$\text{CO}_3^- + \text{H}_2\text{O} + \text{M}$	\rightarrow	$\text{CO}_3^- (\text{H}_2\text{O}) + \text{M}$	1.0×10^{-28}	Kazil [2002]
41	$\text{CO}_3^- + \text{Cl}$	\rightarrow	$\text{Cl}^- + \text{CO}_2 + \text{O}$	1.0×10^{-10}	Turco [1977]
42	$\text{CO}_3^- + \text{ClO}$	\rightarrow	$\text{ClO}^- + \text{CO}_2$	1.0×10^{-10}	Turco [1977]
43	$\text{CO}_3^- + \text{ClO}$	\rightarrow	$\text{Cl}^- + \text{CO}_2 + \text{O}_2$	1.0×10^{-11}	Turco [1977]
44	$\text{CO}_3^- + \text{HNO}_3$	\rightarrow	$\text{NO}_3^- + \text{CO}_2 + \text{OH}$	3.51×10^{-10}	Möhler and Arnold [1991]
45	$\text{CO}_4^- + \text{O}_3$	\rightarrow	$\text{O}_3^- + \text{O}_2 + \text{CO}_2$	1.3×10^{-10}	Ikezoe et al. [1987]
46	$\text{CO}_4^- + \text{H}$	\rightarrow	$\text{CO}_3^- + \text{OH}$	2.2×10^{-10}	Ikezoe et al. [1987]
47	$\text{CO}_4^- + \text{O}$	\rightarrow	$\text{CO}_3^- + \text{O}_2$	1.4×10^{-10}	Ikezoe et al. [1987]
48	$\text{CO}_4^- + \text{HCl}$	\rightarrow	$\text{Cl}^- + \text{HO}_2 + \text{CO}_2$	1.2×10^{-9}	Dotan et al. [1978]
49	$\text{CO}_4^- + \text{Cl}$	\rightarrow	$\text{Cl}^- + \text{CO}_2 + \text{O}_2$	1.0×10^{-10}	Turco [1977]
50	$\text{CO}_4^- + \text{ClO}$	\rightarrow	$\text{ClO}^- + \text{CO}_2 + \text{O}_2$	1.0×10^{-10}	Turco [1977]
51	$\text{NO}_2^- + \text{H}$	\rightarrow	$\text{OH}^- + \text{NO}$	3.0×10^{-10}	Ikezoe et al. [1987]
52	$\text{NO}_2^- + \text{NO}_2$	\rightarrow	$\text{NO}_3^- + \text{NO}$	2.0×10^{-13}	Albritton [1978]
53	$\text{NO}_2^- + \text{O}_3$	\rightarrow	$\text{NO}_3^- + \text{O}_2$	1.2×10^{-10}	Ikezoe et al. [1987]
54	$\text{NO}_2^- + \text{HCl}$	\rightarrow	$\text{Cl}^- + \text{HNO}_2$	1.4×10^{-9}	Ikezoe et al. [1987]
55	$\text{NO}_2^- + \text{Cl}$	\rightarrow	$\text{Cl}^- + \text{NO}_2$	1.0×10^{-10}	Turco [1977]
56	$\text{NO}_2^- + \text{ClO}$	\rightarrow	$\text{Cl}^- + \text{NO}_3$	1.0×10^{-10}	Turco [1977]
57	$\text{NO}_2^- + \text{H}_2\text{O} + \text{M}$	\rightarrow	$\text{NO}_2^- (\text{H}_2\text{O}) + \text{M}$	1.6×10^{-28}	Albritton [1978]
58	$\text{NO}_2^- + \text{HNO}_3$	\rightarrow	$\text{NO}_3^- + \text{HNO}_2$	1.6×10^{-9}	Ikezoe et al. [1987]
59	$\text{NO}_3^- + \text{O}$	\rightarrow	$\text{NO}_2^- + \text{O}_2$	0.5×10^{-11}	Albritton [1978]
60	$\text{NO}_3^- + \text{O}_3$	\rightarrow	$\text{NO}_3^- + 2\text{O}_2$	1.0×10^{-13}	Albritton [1978]
61	$\text{NO}_3^- + \text{HCl} + \text{M}$	\rightarrow	$\text{NO}_3^- (\text{HCl}) + \text{M}$	$5.22 \times 10^{-28} \times (300/T)^{2.62}$	Ikezoe et al. [1987]
62	$\text{NO}_3^- + \text{H}_2\text{O} + \text{M}$	\rightarrow	$\text{NO}_3^- (\text{H}_2\text{O}) + \text{M}$	1.6×10^{-28}	Kazil [2002]
63	$\text{NO}_3^- + \text{HNO}_3 + \text{M}$	\rightarrow	$\text{NO}_3^- (\text{HNO}_3) + \text{M}$	1.45×10^{-26}	Möhler and Arnold [1991]
64	$\text{NO}_3^- + \text{HCl}$	\rightarrow	$\text{Cl}^- + \text{HNO}_3$	1.0×10^{-12}	Ikezoe et al. [1987]
65	$\text{Cl}^- + \text{NO}_2$	\rightarrow	$\text{NO}_2^- + \text{Cl}$	6.0×10^{-12}	Kopp [1996]
66	$\text{Cl}^- + \text{H}_2\text{O} + \text{M}$	\rightarrow	$\text{Cl}^- (\text{H}_2\text{O}) + \text{M}$	2.0×10^{-29}	Turco [1977]
67	$\text{Cl}^- (\text{H}_2\text{O}) + \text{M}$	\rightarrow	$\text{Cl}^- + \text{H}_2\text{O} + \text{M}$	$2.0 \times 10^{-8} \times e^{-6600/T}$	Turco [1977]
68	$\text{Cl}^- + \text{HNO}_3$	\rightarrow	$\text{NO}_3^- + \text{HCl}$	2.8×10^{-9}	Huey [1996]
69	$\text{Cl}^- + \text{HCl} + \text{M}$	\rightarrow	$\text{Cl}^- (\text{HCl}) + \text{M}$	1.0×10^{-27}	Kazil [2002]
70	$\text{Cl}^- (\text{H}_2\text{O}) + \text{HCl}$	\rightarrow	$\text{Cl}^- (\text{HCl}) + \text{H}_2\text{O}$	1.30×10^{-9}	Amelynck et al. [1998]
71	$\text{Cl}^- (\text{HCl}) + \text{M}$	\rightarrow	$\text{Cl}^- + \text{HCl} + \text{M}$	$3.33 \times 10^{-3} \times (300/T) \times e^{-11926/T}$	Meot-Ner and Lias [2000]
72	$\text{ClO}^- + \text{NO}$	\rightarrow	$\text{NO}_2^- + \text{Cl}$	2.9×10^{-12}	Turco [1977]
73	$\text{ClO}^- + \text{NO}$	\rightarrow	$\text{Cl}^- + \text{NO}_2$	2.9×10^{-11}	Turco [1977]
74	$\text{ClO}^- + \text{O}$	\rightarrow	$\text{Cl}^- + \text{O}_2$	2.0×10^{-10}	Turco [1977]
75	$\text{CO}_3^- (\text{H}_2\text{O}) + \text{NO}$	\rightarrow	$\text{NO}_2^- + \text{H}_2\text{O} + \text{CO}_2$	3.5×10^{-12}	Ikezoe et al. [1987]
76	$\text{CO}_3^- (\text{H}_2\text{O}) + \text{NO}_2$	\rightarrow	$\text{NO}_3^- + \text{H}_2\text{O} + \text{CO}_2$	4.0×10^{-11}	Arnold et al. [1995]
77	$\text{CO}_3^- (\text{H}_2\text{O}) + \text{M}$	\rightarrow	$\text{CO}_3^- + \text{H}_2\text{O} + \text{M}$	$7.2 \times 10^{-4} \times (300/T) \times e^{-7050/T}$	Keesee et al. [1979]
78	$\text{CO}_3^- (\text{H}_2\text{O}) + \text{NO}_2$	\rightarrow	$\text{NO}_3^- (\text{H}_2\text{O}) + \text{CO}_2$	4.0×10^{-11}	Arnold et al. [1995]
79	$\text{CO}_3^- (\text{H}_2\text{O}) + \text{H}_2\text{O} + \text{M}$	\rightarrow	$\text{CO}_3^- (\text{H}_2\text{O})_2 + \text{M}$	1.0×10^{-28}	Kazil [2002]
80	$\text{CO}_3^- (\text{H}_2\text{O}) + \text{NO}$	\rightarrow	$\text{NO}_2^- (\text{H}_2\text{O}) + \text{CO}_2$	3.5×10^{-12}	Ikezoe et al. [1987]
81	$\text{CO}_3^- (\text{H}_2\text{O})_2 + \text{M}$	\rightarrow	$\text{CO}_3^- (\text{H}_2\text{O}) + \text{H}_2\text{O} + \text{M}$	$6.5 \times 10^{-3} \times (300/T) \times e^{-6800/T}$	Keesee et al. [1979]
82	$\text{NO}_2^- (\text{H}_2\text{O}) + \text{M}$	\rightarrow	$\text{NO}_2^- + \text{H}_2\text{O} + \text{M}$	$5.7 \times 10^{-4} \times (300/T) \times e^{-7600/T}$	Lee et al. [1980]
83	$\text{NO}_3^- (\text{H}_2\text{O}) + \text{H}_2\text{O} + \text{M}$	\rightarrow	$\text{NO}_3^- (\text{H}_2\text{O})_2 + \text{M}$	1.6×10^{-28}	Kazil [2002]
84	$\text{NO}_3^- (\text{H}_2\text{O}) + \text{N}_2\text{O}_5$	\rightarrow	$\text{NO}_3^- (\text{HNO}_3) + \text{HNO}_3$	7.0×10^{-10}	Wincel et al. [1995]
85	$\text{NO}_3^- (\text{H}_2\text{O}) + \text{HNO}_3$	\rightarrow	$\text{NO}_3^- (\text{HNO}_3) + \text{H}_2\text{O}$	1.6×10^{-9}	Möhler and Arnold [1991]
86	$\text{NO}_3^- (\text{H}_2\text{O}) + \text{M}$	\rightarrow	$\text{NO}_3^- + \text{H}_2\text{O} + \text{M}$	$1.0 \times 10^{-3} \times (300/T) \times e^{-7300/T}$	Lee et al. [1980]
87	$\text{NO}_3^- (\text{H}_2\text{O})_2 + \text{M}$	\rightarrow	$\text{NO}_3^- (\text{H}_2\text{O}) + \text{H}_2\text{O} + \text{M}$	$1.5 \times 10^{-2} \times (300/T) \times e^{-7150/T}$	Lee et al. [1980]
88	$\text{NO}_3^- (\text{H}_2\text{O})_2 + \text{N}_2\text{O}_5$	\rightarrow	$\text{NO}_3^- (\text{HNO}_3) + \text{HNO}_3 + \text{H}_2\text{O}$	7.0×10^{-10}	Wincel et al. [1995]
89	$\text{NO}_3^- (\text{HCl}) + \text{HNO}_3$	\rightarrow	$\text{NO}_3^- (\text{HNO}_3) + \text{HCl}$	7.6×10^{-10}	Amelynck et al. [1994]
90	$\text{NO}_3^- (\text{HNO}_3) + \text{M}$	\rightarrow	$\text{NO}_3^- + \text{HNO}_3 + \text{M}$	$6 \times 10^{-3} \times (300/T) \times e^{-13130/T}$	Lee et al. [1980]

A2.6. Electron Detachment From Negative Ions (EDN)

Nr	Reactants	Products	Reaction Rate Coefficient	Source
1	$O^- + O$	$\rightarrow O_2 + e$	1.9×10^{-10}	Albritton [1978]
2	$O^- + NO$	$\rightarrow NO_2 + e$	$3.1 \times 10^{-10} \times (300/T)^{0.83}$	Viggiano and Paulson [1984]
3	$O^- + O_2(^1\Delta_g)$	$\rightarrow O_3 + e$	3.0×10^{-10}	Albritton [1978]
4	$O^- + M$	$\rightarrow O + M + e$	0.5×10^{-12}	Albritton [1978]
5	$O^- + H_2$	$\rightarrow H_2O + e$	6.0×10^{-10}	Ikezoe et al. [1987]
6	$O_2^- + O$	$\rightarrow O_3 + e$	1.5×10^{-10}	Albritton [1978]
7	$O_2^- + O_2(^1\Delta_g)$	$\rightarrow 2O_2 + e$	2.0×10^{-10}	Albritton [1978]
8	$O_2^- + N_2$	$\rightarrow N_2 + O_2 + e$	$1.9 \times 10^{-12} \times (300/T)^{-1.5} \times e^{-4990/T}$	Phelps [1969]
9	$O_2^- + H$	$\rightarrow HO_2 + e$	1.4×10^{-9}	Brasseur and Baets [1986]
10	$O_3^- + O$	$\rightarrow 2O_2 + e$	1.0×10^{-10}	LeVier and Branscomb [1968]
11	$O_3^- + O_3$	$\rightarrow 3O_2 + e$	1.0×10^{-10}	Adams and Megill [1967]
12	$OH^- + O$	$\rightarrow HO_2 + e$	2.0×10^{-10}	Albritton [1978]
13	$OH^- + H$	$\rightarrow H_2O + e$	1.4×10^{-9}	Albritton [1978]
14	$Cl^- + H$	$\rightarrow HCl + e$	9.6×10^{-10}	Turco [1977]

A2.7. Photodetachment of Electrons From Negative Ions (EPN)

Nr	Reactants	Products	Reaction Rate Coefficient	Source
1	$O^- + h\nu$	$\rightarrow O + e$	1.4	Phelps [1969]
2	$O_2^- + h\nu$	$\rightarrow O_2 + e$	3.8×10^{-1}	Phelps [1969]
3	$O_3^- + h\nu$	$\rightarrow O_3 + e$	4.7×10^{-2}	Cosby et al. [1976]
4	$OH^- + h\nu$	$\rightarrow OH + e$	1.1	Cosby et al. [1976]
5	$NO_2^- + h\nu$	$\rightarrow NO_2 + e$	8.0×10^{-4}	Dunkin et al. [1971]
6	$NO_3^- + h\nu$	$\rightarrow NO_3 + e$	5.2×10^{-2}	Smith et al. [1979]

A2.8. Negative Ion Photodissociation (PNI)

Nr	Reactants	Products	Reaction Rate Coefficient	Source
1	$O_3^- + h\nu$	$\rightarrow O^- + O_2$	0.47	Bortner and Baurer [1972]
2	$O_4^- + h\nu$	$\rightarrow O_2^- + O_2$	0.24	Bortner and Baurer [1972]
3	$CO_3^- + h\nu$	$\rightarrow O^- + CO_2$	0.15	Moseley et al. [1976]
4	$CO_4^- + h\nu$	$\rightarrow O_2^- + CO_2$	6.2×10^{-3}	Cosby et al. [1976]
5	$CO_3^-(H_2O) + h\nu$	$\rightarrow CO_3^- + H_2O$	6.0×10^{-1}	Wisemberg and Kockarts [1980]

A2.9. Ion-Ion Recombination (IIR), Two-Body Reaction

Nr	Reactants	Products	Reaction Rate Coefficient	Source
1	$H^+(H_2O)_4 + NO_3^-(HNO_3)$	$\rightarrow 2HNO_3 + 4H_2O$	$6.0 \times 10^{-8} \times (300/T)^{0.5a}$	Arijs et al. [1987]
2	$H^+(H_2O)_4 + CO_3^-$	$\rightarrow H + 4H_2O + O + CO_2$		
3	$H^+(H_2O)_4 + Cl^- (HCl)$	$\rightarrow H + 4H_2O + Cl + HCl$		
4	$H^+(H_2O)_4 + NO_3^-$	$\rightarrow HNO_3 + 4H_2O$		
5	$H^+(H_2O)_4 + HCO_3^-$	$\rightarrow H + 4H_2O + OH + CO_2$		
6	$H^+(H_2O)_4 + O_2^-$	$\rightarrow H + 4H_2O + O_2$		
7	$H^+(H_2O)_4 + CO_4^-$	$\rightarrow H + 4H_2O + O_2 + CO_2$		
8	$H^+(H_2O)_4 + NO_3^-(H_2O)$	$\rightarrow H + 5H_2O + NO_3$		
9	$H^+(H_2O)_4 + CO_3^-(H_2O)_2$	$\rightarrow H + 6H_2O + O + CO_2$		
10	$H^+(H_2O)_4 + Cl^-$	$\rightarrow H + 4H_2O + Cl$		
11	$H^+(H_2O)_4 + CO_3^-(H_2O)$	$\rightarrow H + 5H_2O + O + CO_2$		
12	$H^+(H_2O)_4 + NO_2^-(H_2O)$	$\rightarrow H + 5H_2O + NO_2$		
13	$H^+(H_2O)_4 + NO_3^-(HCl)$	$\rightarrow H + 4H_2O + NO_3 + HCl$		
14	$H^+(H_2O)_4 + Cl^- (H_2O)$	$\rightarrow H + 5H_2O + Cl$		
15	$H^+(H_2O)_4 + NO_3^-(H_2O)_2$	$\rightarrow H + 6H_2O + NO_3$		
16	$H^+(H_2O)_4 + NO_2^-$	$\rightarrow H + 4H_2O + NO_2$		

(continued)

Table (continued)

17	$H^+(H_2O)_5 + NO_3^- (HNO_3)$	→	$2^*HNO_3 + 5H_2O$		
18	$H^+(H_2O)_5 + CO_3^-$	→	$H + 5H_2O + O + CO_2$		
19	$H^+(H_2O)_5 + Cl^- (HCl)$	→	$H + 5H_2O + Cl + HCl$		
20	$H^+(H_2O)_5 + NO_3^-$	→	$HNO_3 + 5H_2O$		
21	$H^+(H_2O)_5 + HCO_3^-$	→	$H + 5H_2O + OH + CO_2$		
22	$H^+(H_2O)_5 + O_2^-$	→	$H + 5H_2O + O_2$		
23	$H^+(H_2O)_5 + CO_4^-$	→	$H + 5H_2O + O_2 + CO_2$		
24	$H^+(H_2O)_5 + NO_3^- (H_2O)$	→	$H + 6H_2O + NO_3$		
25	$H^+(H_2O)_5 + CO_3^- (H_2O)_2$	→	$H + 7H_2O + O + CO_2$		
26	$H^+(H_2O)_5 + Cl^-$	→	$H + 5H_2O + Cl$		
27	$H^+(H_2O)_5 + CO_3^- (H_2O)$	→	$H + 6H_2O + O + CO_2$		
28	$H^+(H_2O)_5 + NO_2^- (H_2O)$	→	$H + 6H_2O + NO_2$		
29	$H^+(H_2O)_5 + NO_3^- (HCl)$	→	$H + 5H_2O + NO_3 + HCl$		
30	$H^+(H_2O)_5 + Cl^- (H_2O)$	→	$H + 6H_2O + Cl$		
31	$H^+(H_2O)_5 + NO_3^- (H_2O)_2$	→	$H + 7H_2O + NO_3$		
32	$H^+(H_2O)_5 + NO_2^-$	→	$H + 5H_2O + NO_2$		
33	$H^+(H_2O)_3 + NO_3^- (HNO_3)$	→	$2HNO_3 + 3H_2O$		
34	$H^+(H_2O)_3 + CO_3^-$	→	$H + 3H_2O + O + CO_2$		
35	$H^+(H_2O)_3 + Cl^- (HCl)$	→	$H + 3H_2O + Cl + HCl$		
36	$H^+(H_2O)_3 + NO_3^-$	→	$HNO_3 + 3H_2O$		
37	$H^+(H_2O)_3 + HCO_3^-$	→	$H + 3H_2O + OH + CO_2$		
38	$H^+(H_2O)_3 + O_2^-$	→	$H + 3H_2O + O_2$		
39	$H^+(H_2O)_3 + CO_4^-$	→	$H + 3H_2O + O_2 + CO_2$		
40	$H^+(H_2O)_3 + NO_3^- (H_2O)$	→	$H + 4H_2O + NO_3$		
41	$H^+(H_2O)_3 + CO_3^- (H_2O)_2$	→	$H + 5H_2O + O + CO_2$		
42	$H^+(H_2O)_3 + Cl^-$	→	$H + 3H_2O + Cl$		
43	$H^+(H_2O)_3 + CO_3^- (H_2O)$	→	$H + 4H_2O + O + CO_2$		
44	$H^+(H_2O)_3 + NO_2^- (H_2O)$	→	$H + 4H_2O + NO_2$		
45	$H^+(H_2O)_3 + NO_3^- (HCl)$	→	$H + 3H_2O + NO_3 + HCl$		
46	$H^+(H_2O)_3 + Cl^- (H_2O)$	→	$H + 4H_2O + Cl$		
47	$H^+(H_2O)_3 + NO_3^- (H_2O)_2$	→	$H + 5H_2O + NO_3$		
48	$H^+(H_2O)_3 + NO_2^-$	→	$H + 3H_2O + NO_2$		
49	$NO^+(H_2O) + NO_3^- (HNO_3)$	→	$NO + H_2O + NO_3 + HNO_3$		
50	$NO^+(H_2O) + CO_3^-$	→	$NO + H_2O + O + CO_2$		
51	$NO^+(H_2O) + Cl^- (HCl)$	→	$NO + H_2O + Cl + HCl$	$6.0 \times 10^{-8} \times (300/T)^{0.5a}$	Arijs et al. [1987]
52	$NO^+(H_2O) + NO_3^-$	→	$NO + H_2O + NO_3$		
53	$NO^+(H_2O) + HCO_3^-$	→	$NO + H_2O + OH + CO_2$		
54	$NO^+(H_2O) + O_2^-$	→	$NO + H_2O + O_2$		
55	$NO^+(H_2O) + CO_4^-$	→	$NO + H_2O + O_2 + CO_2$		
56	$NO^+(H_2O) + NO_3^- (H_2O)$	→	$NO + 2H_2O + NO_3$		
57	$NO^+(H_2O) + CO_3^- (H_2O)_2$	→	$NO + 3H_2O + O + CO_2$		
58	$NO^+(H_2O) + Cl^-$	→	$NO + H_2O + Cl$		
59	$NO^+(H_2O) + CO_3^- (H_2O)$	→	$NO + 2H_2O + O + CO_2$		
60	$NO^+(H_2O) + NO_2^- (H_2O)$	→	$NO + 2H_2O + NO_2$		
61	$NO^+(H_2O) + NO_3^- (HCl)$	→	$NO + H_2O + NO_3 + HCl$		
62	$NO^+(H_2O) + Cl^- (H_2O)$	→	$NO + 2H_2O + Cl$		
63	$NO^+(H_2O) + NO_3^- (H_2O)_2$	→	$NO + 3H_2O + NO_3$		
64	$NO^+(H_2O) + NO_2^-$	→	$NO + H_2O + NO_2$		
65	$NO^+(H_2O)_2 + NO_3^- (HNO_3)$	→	$NO + 2H_2O + NO_3 + HNO_3$		
66	$NO^+(H_2O)_2 + CO_3^-$	→	$NO + 2H_2O + O + CO_2$		
67	$NO^+(H_2O)_2 + Cl^- (HCl)$	→	$NO + 2H_2O + Cl + HCl$		
68	$NO^+(H_2O)_2 + NO_3^-$	→	$NO + 2H_2O + NO_3$		
69	$NO^+(H_2O)_2 + HCO_3^-$	→	$NO + 2H_2O + OH + CO_2$		
70	$NO^+(H_2O)_2 + O_2^-$	→	$NO + 2H_2O + O_2$		
71	$NO^+(H_2O)_2 + CO_4^-$	→	$NO + 2H_2O + O_2 + CO_2$		
72	$NO^+(H_2O)_2 + NO_3^- (H_2O)$	→	$NO + 3H_2O + NO_3$		
73	$NO^+(H_2O)_2 + CO_3^- (H_2O)_2$	→	$NO + 4H_2O + O + CO_2$		
74	$NO^+(H_2O)_2 + Cl^-$	→	$NO + 2H_2O + Cl$		
75	$NO^+(H_2O)_2 + CO_3^- (H_2O)$	→	$NO + 3H_2O + O + CO_2$		
76	$NO^+(H_2O)_2 + NO_2^- (H_2O)$	→	$NO + 3H_2O + NO_2$		
77	$NO^+(H_2O)_2 + NO_3^- (HCl)$	→	$NO + 2H_2O + NO_3 + HCl$		
78	$NO^+(H_2O)_2 + Cl^- (H_2O)$	→	$NO + 3H_2O + Cl$		
79	$NO^+(H_2O)_2 + NO_3^- (H_2O)_2$	→	$NO + 4H_2O + NO_3$		
80	$NO^+(H_2O)_2 + NO_2^-$	→	$NO + 2H_2O + NO_2$		
81	$NO^+ + NO_3^- (HNO_3)$	→	$NO + NO_3 + HNO_3$		
82	$NO^+ + CO_3^-$	→	$NO + O + CO_2$		
83	$NO^+ + Cl^- (HCl)$	→	$NO + Cl + HCl$		
84	$NO^+ + NO_3^-$	→	$NO + NO_3$		
85	$NO^+ + HCO_3^-$	→	$NO + OH + CO_2$		

(continued)

Table (continued)

86	$\text{NO}^+ + \text{O}_2^-$	→	$\text{NO} + \text{O}_2$		
87	$\text{NO}^+ + \text{CO}_4^-$	→	$\text{NO} + \text{O}_2 + \text{CO}_2$		
88	$\text{NO}^+ + \text{NO}_3^- (\text{H}_2\text{O})$	→	$\text{NO} + \text{NO}_3 + \text{H}_2\text{O}$		
89	$\text{NO}^+ + \text{CO}_3^- (\text{H}_2\text{O})_2$	→	$\text{NO} + \text{O} + 2\text{H}_2\text{O} + \text{CO}_2$		
90	$\text{NO}^+ + \text{Cl}^-$	→	$\text{NO} + \text{Cl}$		
91	$\text{NO}^+ + \text{CO}_3^- (\text{H}_2\text{O})$	→	$\text{NO} + \text{O} + \text{H}_2\text{O} + \text{CO}_2$		
92	$\text{NO}^+ + \text{NO}_2^- (\text{H}_2\text{O})$	→	$\text{NO} + \text{NO}_2 + \text{H}_2\text{O}$		
93	$\text{NO}^+ + \text{NO}_3^- (\text{HCl})$	→	$\text{NO} + \text{NO}_3 + \text{HCl}$		
94	$\text{NO}^+ + \text{Cl}^- (\text{H}_2\text{O})$	→	$\text{NO} + \text{Cl} + \text{H}_2\text{O}$		
95	$\text{NO}^+ + \text{NO}_3^- (\text{H}_2\text{O})_2$	→	$\text{NO} + \text{NO}_3 + 2\text{H}_2\text{O}$		
96	$\text{NO}^+ + \text{NO}_2^-$	→	$\text{NO} + \text{NO}_2$		
97	$\text{O}_2^+ + \text{NO}_3^- (\text{HNO}_3)$	→	$\text{O}_2 + \text{NO}_3 + \text{HNO}_3$		
98	$\text{O}_2^+ + \text{CO}_3^-$	→	$\text{O}_2 + \text{O} + \text{CO}_2$		
99	$\text{O}_2^+ + \text{Cl}^- (\text{HCl})$	→	$\text{O}_2 + \text{Cl} + \text{HCl}$		
100	$\text{O}_2^+ + \text{NO}_3^-$	→	$\text{O}_2 + \text{NO}_3$		
101	$\text{O}_2^+ + \text{HCO}_3^-$	→	$\text{O}_2 + \text{OH} + \text{CO}_2$	$6.0 \times 10^{-8} \times (300/T)^{0.5a}$	Arijs et al. [1987]
102	$\text{O}_2^+ + \text{O}_2^-$	→	2O_2^+		
103	$\text{O}_2^+ + \text{CO}_4^-$	→	$\text{O}_2 + \text{O}_2 + \text{CO}_2$		
104	$\text{O}_2^+ + \text{NO}_3^- (\text{H}_2\text{O})$	→	$\text{O}_2 + \text{NO}_3 + \text{H}_2\text{O}$		
105	$\text{O}_2^+ + \text{CO}_3^- (\text{H}_2\text{O})_2$	→	$\text{O}_2 + \text{O} + 2\text{H}_2\text{O} + \text{CO}_2$		
106	$\text{O}_2^+ + \text{Cl}^-$	→	$\text{O}_2 + \text{Cl}$		
107	$\text{O}_2^+ + \text{CO}_3^- (\text{H}_2\text{O})$	→	$\text{O}_2 + \text{O} + \text{H}_2\text{O} + \text{CO}_2$		
108	$\text{O}_2^+ + \text{NO}_2^- (\text{H}_2\text{O})$	→	$\text{O}_2 + \text{NO}_2 + \text{H}_2\text{O}$		
109	$\text{O}_2^+ + \text{NO}_3^- (\text{HCl})$	→	$\text{O}_2 + \text{NO}_3 + \text{HCl}$		
110	$\text{O}_2^+ + \text{Cl}^- (\text{H}_2\text{O})$	→	$\text{O}_2 + \text{Cl} + \text{H}_2\text{O}$		
111	$\text{O}_2^+ + \text{NO}_3^- (\text{H}_2\text{O})_2$	→	$\text{O}_2 + \text{NO}_3 + 2\text{H}_2\text{O}$		
112	$\text{O}_2^+ + \text{NO}_2^-$	→	$\text{O}_2 + \text{NO}_2$		

A2.10. Ion-Ion Recombination (IIR), Three-Body Reactions

Nr	Reactants	Products	Reaction Rate Coefficient	Source	
1	$\text{H}^+ (\text{H}_2\text{O})_4 + \text{CO}_3^- + \text{M}$	→	$\text{H} + 4\text{H}_2\text{O} + \text{O} + \text{CO}_2 + \text{M}$	$1.25 \times 10^{-25} \times (300/T)^4 \text{ }^{\text{a}}$	Arijs et al. [1987]
2	$\text{H}^+ (\text{H}_2\text{O})_4 + \text{NO}_3^- + \text{M}$	→	$\text{HNO}_3 + 4\text{H}_2\text{O} + \text{M}$		
3	$\text{H}^+ (\text{H}_2\text{O})_5 + \text{CO}_3^- + \text{M}$	→	$\text{H} + 5\text{H}_2\text{O} + \text{O} + \text{CO}_2 + \text{M}$		
4	$\text{H}^+ (\text{H}_2\text{O})_5 + \text{NO}_3^- + \text{M}$	→	$\text{HNO}_3 + 5\text{H}_2\text{O} + \text{M}$		
5	$\text{H}^+ (\text{H}_2\text{O})_4 + \text{Cl}^- (\text{HCl}) + \text{M}$	→	$2^* \text{HCl} + 4\text{H}_2\text{O} + \text{M}$		
6	$\text{H}^+ (\text{H}_2\text{O})_5 + \text{Cl}^- (\text{HCl}) + \text{M}$	→	$2^* \text{HCl} + 5\text{H}_2\text{O} + \text{M}$		
7	$\text{H}^+ (\text{H}_2\text{O})_4 + \text{NO}_3^- (\text{HNO}_3) + \text{M}$	→	$2^* \text{HNO}_3 + 4\text{H}_2\text{O} + \text{M}$		
8	$\text{H}^+ (\text{H}_2\text{O})_5 + \text{NO}_3^- (\text{HNO}_3) + \text{M}$	→	$2^* \text{HNO}_3 + 5\text{H}_2\text{O} + \text{M}$		
9	$\text{H}^+ (\text{H}_2\text{O})_4 + \text{CO}_3^- (\text{H}_2\text{O})_2 + \text{M}$	→	$\text{H} + 6\text{H}_2\text{O} + \text{O} + \text{CO}_2 + \text{M}$		
10	$\text{H}^+ (\text{H}_2\text{O})_5 + \text{CO}_3^- (\text{H}_2\text{O})_2 + \text{M}$	→	$\text{H} + 7\text{H}_2\text{O} + \text{O} + \text{CO}_2 + \text{M}$		
11	$\text{H}^+ (\text{H}_2\text{O})_4 + \text{CO}_3^- (\text{H}_2\text{O}) + \text{M}$	→	$\text{H} + 5\text{H}_2\text{O} + \text{O} + \text{CO}_2 + \text{M}$		
12	$\text{H}^+ (\text{H}_2\text{O})_5 + \text{CO}_3^- (\text{H}_2\text{O}) + \text{M}$	→	$\text{H} + 6\text{H}_2\text{O} + \text{O} + \text{CO}_2 + \text{M}$		
13	$\text{H}^+ (\text{H}_2\text{O})_4 + \text{NO}_3^- (\text{H}_2\text{O}) + \text{M}$	→	$\text{H} + 5\text{H}_2\text{O} + \text{NO}_3 + \text{M}$		
14	$\text{H}^+ (\text{H}_2\text{O})_5 + \text{NO}_3^- (\text{H}_2\text{O}) + \text{M}$	→	$\text{H} + 6\text{H}_2\text{O} + \text{NO}_3 + \text{M}$		

^aThe coefficient is the same for all reactions.

References

- Adams, G. W., and L. R. Megill (1967), A two ion D-region model for polar cap absorption events, *Planet. Space Sci.*, 15, 1111–1130.
- Albritton, D. L. (1978), Ion-neutral reaction rate constants measured in flow reactors through 1977, *At. Data Nucl. Data Tables*, 22, 1–89, doi: 10.1016/0092-640X(78)90027-X.
- Amelynck, C., D. Fussen, and E. Arijs (1994), Reactions of nitric acid with di- and trichloride ions, di- and tri-iodide ions and with CO_4^- in the gas phase, *Int. J. Mass Spectrom. Ion Processes*, 133, 13–28.
- Amelynck, C., E. Arijs, N. Schoon, and A.-M. V. Bavel (1998), Gas phase reactions of HNO_3 with Cl^- , $\text{Cl}^- \text{H}_2\text{O}$, and $\text{Cl}^- \text{HCl}$, of Cl_2 with $\text{Cl}^- \text{H}_2\text{O}$ and $\text{Cl}^- \text{HCl}$, and of HCl with $\text{Cl}^- \text{H}_2\text{O}$, *Int. J. Mass Spectrom. Ion Processes*, 181, 113–121.
- Andersson, M. E., P. T. Verronen, C. J. Rodger, M. A. Clilverd, and A. Seppälä (2014), Missing driver in the Sun-Earth connection from energetic electron precipitation impacts mesospheric ozone, *Nat. Commun.*, 5, 5197, doi:10.1038/ncomms6197.
- Arijs, E., D. Nevejans, and J. Ingels (1987), Stratospheric positive ion composition measurements and acetonitrile detection: A consistent picture?, *Int. J. Mass Spectrom. Ion Processes*, 81, 15–31.

Acknowledgments

P.T.V. and M.E.A. are supported by the Academy of Finland through the project #276926 (SECTIC: Sun-Earth Connection Through Ion Chemistry). D.R.M. is supported in part by NASA Living With a Star grant NNX14AH54G. The National Center for Atmospheric Research is operated by the University Corporation for Atmospheric Research under sponsorship of the National Science Foundation. T.K. and J.M.C.P. are supported by the UK Natural Environment Research Council (grant NE/J02077X/1). D.R.M. and P.T.V. would like to thank the International Space Science Institute, Bern, Switzerland for supporting the “Quantifying Hemispheric Differences in Particle Forcing Effects on Stratospheric Ozone” team. Data used in this study are available upon request from the corresponding author.

- Arnold, S. T., R. A. Morris, and A. A. Viggiano (1995), Temperature dependencies of the reactions of $\text{CO}_3^- (\text{H}_2\text{O})_{0,1}$ and O_3^- with NO and NO_2 , *J. Chem. Phys.*, *103*, 2454–2458, doi:10.1063/1.469668.
- Böhrringer, H., and F. Arnold (1982), Temperature dependence of three-body association reactions from 45 to 400 K. The reactions $\text{N}_2^+ + 2\text{N}_2 \rightarrow \text{N}_4^+ + \text{N}_2$ and $\text{O}_2^+ + 2\text{O}_2 \rightarrow \text{O}_4^+ + \text{O}_2$, *J. Chem. Phys.*, *77*, 5534–5541.
- Böhrringer, H., D. W. Fahey, F. C. Fehsenfeld, and E. E. Ferguson (1983), The role of ion-molecule reactions in the conversion of N_2O_5 to HNO_3 in the stratosphere, *Planet. Space Sci.*, *31*, 185–191, doi:10.1016/0032-0633(83)90053-3.
- Bortner, M. H., and T. Baurer (1972), *Defense Nuclear Agency Reaction Rate Handbook*, 2nd ed., General Electric, Santa Barbara, Calif.
- Brasseur, G. P., and P. D. Baets (1986), Ions in the mesosphere and lower thermosphere: A two-dimensional model, *J. Geophys. Res.*, *91*, 4025–4046.
- Cosby, P. C., J. H. Ling, J. R. Peterson, and J. T. Moseley (1976), Photodissociation and photodetachment of molecular negative ions. III. Ions formed in $\text{CO}_2/\text{O}_2/\text{H}_2\text{O}$ mixtures, *J. Chem. Phys.*, *65*(12), 5267–5274.
- Dheandhanoo, S., and R. Johnsen (1983), Laboratory measurements of the association rate coefficients of NO^+ , O_2^+ , N^+ and N_2^+ ions with N_2 and CO_2 at temperatures between 100K and 400K, *Planet. Space Sci.*, *31*, 933–938.
- Dotan, I., D. L. Albritton, F. C. Fehsenfeld, G. E. Streit, and E. E. Ferguson (1978), Rate constants for the reactions of O^- , O_2^- , NO_2^- , CO_3^- , and CO_4^- with HCl and ClO^- with NO, NO_2 , SO_2 and CO_2 at 300K, *J. Chem. Phys.*, *68*(12), 5414–5416.
- Dunkin, D. B., F. C. Fehsenfeld, A. L. Schmeltekopf, and E. E. Ferguson (1971), Three-body association reactions of NO^+ with O_2 , N_2 and CO_2 , *J. Chem. Phys.*, *54*, 711–720.
- Egorova, T., E. Rozanov, Y. Ozolin, A. Shapiro, M. Calisto, T. Peter, and W. Schmutz (2011), The atmospheric effects of October 2003 solar proton event simulated with the chemistry-climate model SOCOL using complete and parameterized ion chemistry, *J. Atmos. Sol. Terr. Phys.*, *73*, 356–365, doi:10.1016/j.jastp.2010.01.009.
- Eyet, N., N. S. Shuman, A. A. Viggiano, J. Troe, R. A. Relp, R. P. Steele, and M. A. Johnson (2011), The importance of $\text{NO}^+ (\text{H}_2\text{O})_4$ in the conversion of $\text{NO}^+ (\text{H}_2\text{O})_n$ to $\text{H}_3\text{O}^+ (\text{H}_2\text{O})_n$: I. Kinetics measurements and statistical rate modeling, *J. Phys. Chem. A*, *115*, 7582–7590.
- Fehsenfeld, F. C., and E. E. Ferguson (1974), Laboratory studies of negative ion reactions with atmospheric constituents, *J. Chem. Phys.*, *61*, 3181–3193.
- Fehsenfeld, F. C., M. Mosesman, and E. E. Ferguson (1971), Ion molecule reactions in O_2^- - H_2O system and NO^+ - H_2O system, *J. Chem. Phys.*, *55*, 2115–2126.
- Fehsenfeld, F. C., C. J. Howard, and A. L. Schmeltekopf (1975), Gas phase ion chemistry of HNO_3 , *J. Chem. Phys.*, *63*, 2835–2841.
- Funke, B., et al. (2011), Composition changes after the “Halloween” solar proton event: The High-Energy Particle Precipitation in the Atmosphere (HEPPA) model versus MIPAS data intercomparison study, *Atmos. Chem. Phys.*, *11*, 9089–9139, doi:10.5194/acp-11-9089-2011.
- Huey, L. G. (1996), The kinetics of the reactions of Cl^- , O^- and O_2^- with HNO_3 : Implications for measurements of HNO_3 in the atmosphere, *Int. J. Mass Spectrom. Ion Processes*, *153*, 145–150.
- Ikezoe, Y., S. Matsuoka, M. Takebe, and A. A. Viggiano (1987), *Gas Phase Ion-Molecule Reaction Rate Constants Through 1986*, Ion React. Res. Group of The Mass Spectrosc. Soc. of Jpn., Tokyo, Japan.
- Jackman, C. H., M. T. DeLand, G. J. Labow, E. L. Fleming, D. K. Weisenstein, M. K. W. Ko, M. Sinnhuber, and J. M. Russell (2005), Neutral atmospheric influences of the solar proton events in October–November 2003, *J. Geophys. Res.*, *110*, A09S27, doi:10.1029/2004JA010888.
- Jackman, C. H., D. R. Marsh, F. M. Vitt, R. R. Garcia, C. E. Randall, E. L. Fleming, and S. M. Frith (2009), Long-term middle atmospheric influence of very large solar proton events, *J. Geophys. Res.*, *114*, D11304, doi:10.1029/2008JD011415.
- Jackman, C. H., et al. (2011), Northern Hemisphere atmospheric influence of the solar proton events and ground level enhancement in January 2005, *Atmos. Chem. Phys.*, *11*, 6153–6166, doi:10.5194/acp-11-6153-2011.
- Jackman, C. H., D. R. Marsh, D. E. Kinnison, C. J. Mertens, and E. L. Fleming (2015), Atmospheric changes caused by galactic cosmic rays over the period 1960–2010, *Atmos. Chem. Phys. Discuss.*, *15*, 33,931–33,966, doi:10.5194/acpd-15-33931-2015.
- Johnsen, R. (1987), Microwave afterglow measurements of the dissociative recombination of molecular ions with electrons, *Int. J. Mass Spectrom. Ion Processes*, *81*, 67–84.
- Kazil, J. (2002), The university of bern atmospheric ion model: Time-dependent ion modeling in the stratosphere, mesosphere, and lower thermosphere, PhD thesis, Univ. of Bern, Bern, Switzerland.
- Keese, R. G., N. Lee, and A. W. Castleman Jr. (1979), Properties of clusters in the gas phase. III. Hydration complexes of CO_3^- and HCO_3^- , *J. Am. Chem. Soc.*, *101*, 2599–2604.
- Kinnison, D. E., et al. (2007), Sensitivity of chemical tracers to meteorological parameters in the MOZART-3 chemical transport model, *J. Geophys. Res.*, *112*, D20302, doi:10.1029/2006JD007879.
- Kopp, E. (1996), *Electron and ion densities, in The Upper Atmosphere: Data Analysis and Interpretation*, edited by W. Dieminger, G. K. Hartmann, and R. Leitinger, pp. 620–630, Springer, Berlin, Germany.
- Krivolutsky, A. A., L. A. Cherepanova, T. Y. Vyushkova, and A. I. Repnev (2015), The three-dimensional global numerical model CHARM-I: The incorporation of processes in the ionospheric D-region, *Geomagn. Aeron.*, *55*, 467–486, doi:10.1134/S0016793215030123.
- Kvissel, O.-K., Y. J. Orsolini, F. Stordal, I. S. A. Isaksen, and M. L. Santee (2012), Formation of stratospheric nitric acid by a hydrated ion cluster reaction: Implications for the effect of energetic particle precipitation on the middle atmosphere, *J. Geophys. Res.*, *117*, D16301, doi:10.1029/2011JD017257.
- Lau, J. K., S. Ikuta, and P. Kebarle (1982), Thermodynamics and kinetics of the gas phase reactions $\text{H}_3\text{O}^+ (\text{H}_2\text{O})_n + \text{H}_2\text{O} \rightarrow \text{H}_3\text{O}^+ (\text{H}_2\text{O})_{n+1}$, *J. Am. Chem. Soc.*, *104*, 1462–1469.
- Lee, N., R. G. Keese, and A. W. Castleman (1980), The properties of clusters in the gas phase. IV. Complexes of H_2O and HNO_x clustering on NO_x^- , *J. Chem. Phys.*, *72*, 1089–1094.
- LeVie, R. E., and L. M. Branscomb (1968), Ion chemistry governing mesospheric electron concentrations, *J. Geophys. Res.*, *73*, 27–41.
- Marsh, D. R., R. R. Garcia, D. E. Kinnison, B. A. Boville, F. Sassi, S. C. Solomon, and K. Matthes (2007), Modeling the whole atmosphere response to solar cycle changes in radiative and geomagnetic forcing, *J. Geophys. Res.*, *112*, D23306, doi:10.1029/2006JD008306.
- Marsh, D. R., M. Mills, D. Kinnison, J.-F. Lamarque, N. Calvo, and L. Polvani (2013), Climate change from 1850 to 2005 simulated in CESM1(WACCM), *J. Clim.*, *26*(19), 7372–7391, doi:10.1175/JCLI-D-12-00558.
- McGowan, J. W., and J. B. A. Mitchell (1984), *Electron-Molecular Positive Ion Recombination, Electron-Molecule Interactions and Their Applications*, edited by L. G. Christophorou, vol. 2, Academic, Orlando, Fla.
- Meot-Ner, M. M., and S. G. Lias (2000), *Binding Energies Between Ions and Molecules, and the Thermochemistry of Cluster Ions*, edited by W. G. Mallard and P. J. Linstrom, NIST Chemistry WebBook, NIST Standard Reference Database 69, Natl. Inst. of Stand. and Technol., Gaithersburg, Md.
- Möhler, O., and F. Arnold (1991), Flow reactor and triple quadrupole mass spectrometer investigations of negative ion reactions involving nitric acid: Implications for atmospheric HNO_3 detection by chemical ionization mass spectrometry, *J. Atmos. Chem.*, *13*, 33–61.

- Moseley, J. T., P. C. Cosby, and J. R. Peterson (1976), Photodissociation spectroscopy of CO_3^- , *J. Chem. Phys.*, *65*(7), 2512–2517.
- Nagy, T., and T. Turanyi (2009), Reduction of very large reaction mechanisms using methods based on simulation error minimization, *Combust. Flame*, *156*, 417–428.
- Neale, R. B., et al. (2012), Description of the NCAR Community Atmosphere Model (CAM 5.0), *Tech. Rep. NCAR/TN-486+STR*, Natl. Cent. for Atmos. Res., Boulder, Colo.
- Öjekull, J., et al. (2007), Dissociative recombination of $\text{H}^+(\text{H}_2\text{O})_3$ and $\text{D}^+(\text{D}_2\text{O})_3$ water cluster ions with electrons: Cross sections and branching ratios, *J. Chem. Phys.*, *127*, 194301.
- Pavlov, A. V. (2013), Photochemistry of ions at D-region altitudes of the ionosphere: A review, *Surv. Geophys.*, *35*, 259–334.
- Payzant, J. D., and P. Kebarle (1972), Kinetics of Reactions Leading to $\text{O}_2^+(\text{H}_2\text{O})_n$ in Moist Oxygen, *J. Comput. Phys.*, *56*, 3482–3487, doi: 10.1063/1.1677723.
- Phelps, A. V. (1969), Laboratory studies of electron attachment and detachment processes of aeronomic interest, *Can. J. Chem.*, *47*, 1783–1793.
- Porter, H. S., C. H. Jackman, and A. E. S. Green (1976), Efficiencies for production of atomic nitrogen and oxygen by relativistic proton impact in air, *J. Chem. Phys.*, *65*, 154–167.
- Rakshit, A. B., and P. Warneck (1980), A drift chamber study of the formation of water cluster ions in oxygen, *J. Chem. Phys.*, *73*(10), 5074–5080.
- Reid, G. C. (1977), The production of water-cluster positive ions in the quiet daytime D-region, *Planet. Space Sci.*, *25*, 275–290.
- Reinecker, M. M., et al. (2008), The GEOS-5 data assimilation system: A documentation of GEOS-5.0, *Tech. Rep. 104606 V27*, NASA Goddard Space Flight Center, Greenbelt, Md.
- Roble, P. B., and E. C. Ridley (1987), An auroral model for the NCAR thermospheric general circulation model (TGCM), *Ann. Geophys., Ser. A*, *5*(6), 369–382.
- Roble, R. G. (1995), Energetics of the mesosphere and thermosphere, in *The Upper Mesosphere and Lower Thermosphere: A Review of Experiment and Theory*, *Geophys. Monogr. Ser.*, vol. 87, edited by R. M. Johnson and K. T. L., pp. 1–21, AGU, Washington, D. C.
- Rusch, D. W., J.-C. Gérard, S. Solomon, P. J. Crutzen, and G. C. Reid (1981), The effect of particle precipitation events on the neutral and ion chemistry of the middle atmosphere—I. Odd nitrogen, *Planet. Space Sci.*, *29*, 767–774.
- Sandu, A., F. A. Potra, G. R. Carmichael, and V. Damian (1996), Efficient implementation of fully implicit methods for atmospheric chemical kinetics, *J. Comput. Phys.*, *129*, 101–110, doi:10.1006/jcph.1996.0236.
- Sinnhuber, M., H. Nieder, and N. Wieters (2012), Energetic particle precipitation and the chemistry of the mesosphere/lower thermosphere, *Surv. Geophys.*, *33*, 1281–1334, doi:10.1007/s10712-012-9201-3.
- Smith, G. P., L. C. Lee, P. C. Cosby, J. R. Peterson, and J. T. Moseley (1978), Photodissociation and photodetachment of molecular negative ions. v. atmospheric ions from 7000 to 8400 Å, *J. Chem. Phys.*, *68*, 3818–3822.
- Smith, G. P., L. C. Lee, and J. T. Moseley (1979), Photodissociation and photodetachment of molecular negative ions. VII. Ions formed in $\text{CO}_2/\text{O}_2/\text{H}_2\text{O}$ mixtures, 3500–5300 Å, *J. Chem. Phys.*, *71*, 4034–4041.
- Solomon, S., D. W. Rusch, J.-C. Gérard, G. C. Reid, and P. J. Crutzen (1981), The effect of particle precipitation events on the neutral and ion chemistry of the middle atmosphere: II. Odd hydrogen, *Planet. Space Sci.*, *8*, 885–893.
- Stelman, D., J. L. Moruzzi, and A. V. Phelps (1972), Low energy electron attachment to ozone using swarm techniques, *J. Chem. Phys.*, *56*, 4183–4189.
- Swider, W., and R. S. Narcisi (1975), A study of the nighttime d-region, *J. Geophys. Res.*, *80*, 655–664.
- Swider, W., and R. S. Narcisi (1983), Steady state model of the D-region during the february 1977 eclipse, *J. Atmos. Terr. Phys.*, *45*, 493–498.
- Thomas, L. (1976), NO^+ and water cluster ions in the D-region, *J. Atmos. Terr. Phys.*, *47*, 61–67.
- Thomas, L., and M. R. Bowman (1985), Model studies of the D-region negative-ion composition during day-time and night-time, *J. Atmos. Terr. Phys.*, *47*, 547–556.
- Truby, F. (1972), Low-temperature measurements of three-body electron-attachment coefficient in O_2 , *Phys. Rev. A*, *6*, 671.
- Turco, R. (1977), On the formation and destruction of chlorine negative ions in the D-region, *J. Geophys. Res.*, *82*, 3585–3592.
- Turunen, E., P. T. Verronen, A. Seppälä, C. J. Rodger, M. A. Clilverd, J. Tamminen, C.-F. Enell, and T. Ulich (2009), Impact of different precipitation energies on NO_x generation during geomagnetic storms, *J. Atmos. Sol. Terr. Phys.*, *71*, 1176–1189, doi:10.1016/j.jastp.2008.07.005.
- Verronen, P. T., and R. Lehmann (2013), Analysis and parameterisation of ionic reactions affecting middle atmospheric HO_x and NO_y during solar proton events, *Ann. Geophys.*, *31*, 909–956, doi:10.5194/angeo-31-909-2013.
- Verronen, P. T., A. Seppälä, M. A. Clilverd, C. J. Rodger, E. Kyrölä, C.-F. Enell, T. Ulich, and E. Turunen (2005), Diurnal variation of ozone depletion during the October–November 2003 solar proton events, *J. Geophys. Res.*, *110*, A09S32, doi:10.1029/2004JA010932.
- Verronen, P. T., A. Seppälä, E. Kyrölä, J. Tamminen, H. M. Pickett, and E. Turunen (2006a), Production of odd hydrogen in the mesosphere during the January 2005 solar proton event, *Geophys. Res. Lett.*, *33*, L24811, doi:10.1029/2006GL028115.
- Verronen, P. T., T. Ulich, E. Turunen, and C. J. Rodger (2006b), Sunset transition of negative charge in the D-region ionosphere during high-ionization conditions, *Ann. Geophys.*, *24*, 187–202.
- Verronen, P. T., B. Funke, M. López-Puertas, G. P. Stiller, T. von Clarmann, N. Glatthor, C.-F. Enell, E. Turunen, and J. Tamminen (2008), About the increase of HNO_3 in the stratopause region during the Halloween 2003 solar proton event, *Geophys. Res. Lett.*, *35*, L20809, doi: 10.1029/2008GL035312.
- Verronen, P. T., M. L. Santee, G. L. Manney, R. Lehmann, S.-M. Salmi, and A. Seppälä (2011), Nitric acid enhancements in the mesosphere during the January 2005 and December 2006 solar proton events, *J. Geophys. Res.*, *116*, D17301, doi:10.1029/2011JD016075.
- Verronen, P. T., M. E. Andersson, A. Kero, C.-F. Enell, J. M. Wissing, E. R. Talaat, K. Kauristie, M. Palmroth, T. E. Sarris, and E. Armandillo (2015), Contribution of proton and electron precipitation to the observed electron concentration in October–November 2003 and September 2005, *Ann. Geophys.*, *33*, 381–394, doi:10.5194/angeo-33-381-2015.
- Viggiano, A. A., and K. F. Paulson (1984), Reactions of negative ions, in *Swarms of Ions and Electrons in Gases*, edited by W. Lindinger, T. D. Märk, and F. Howorka, 218 pp., Springer, Vienna, Austria.
- Wincel, H., E. Mereand, and A. W. Castleman Jr. (1995), Gas phase reactions of N_2O_5 with $\text{NO}_2^- (\text{H}_2\text{O})_{n=0-2}$, $\text{NO}_3^- (\text{H}_2\text{O})_{n=1,2}$, and $\text{NO}_2^-_{n=2,3} \text{HNO}_2$, *J. Chem. Phys.*, *102*(23), 9228–9234.
- Wisemberg, J., and G. Kockarts (1980), Negative ion chemistry in the terrestrial D-region and signal flow graph theory, *J. Geophys. Res.*, *85*, 4642–4652.
- Zipf, E. C., P. J. Espy, and C. F. Boyle (1980), The excitation and collisional deactivation of metastable $\text{N}(^2\text{P})$ atoms in auroras, *J. Geophys. Res.*, *85*, 687–694.